# Low-lying structure of p-sd shell hypernuclei and YN interaction with Antisymmetrized Molecular Dynamics

**Today: not only Λ hypernuclei but also Ξ hypernuclei**

Masahiro Isaka

Hosei University

# Recent developments in hypernuclear physics

## ◆Experiments

### ●Λ hypernuclei

- Mass dependence of $B_\Lambda$
- Level structure
- Future exp at J-PARC, JLab, etc.

O. Hashimoto and H. Tamura, PPNP **57** (2006), 564.

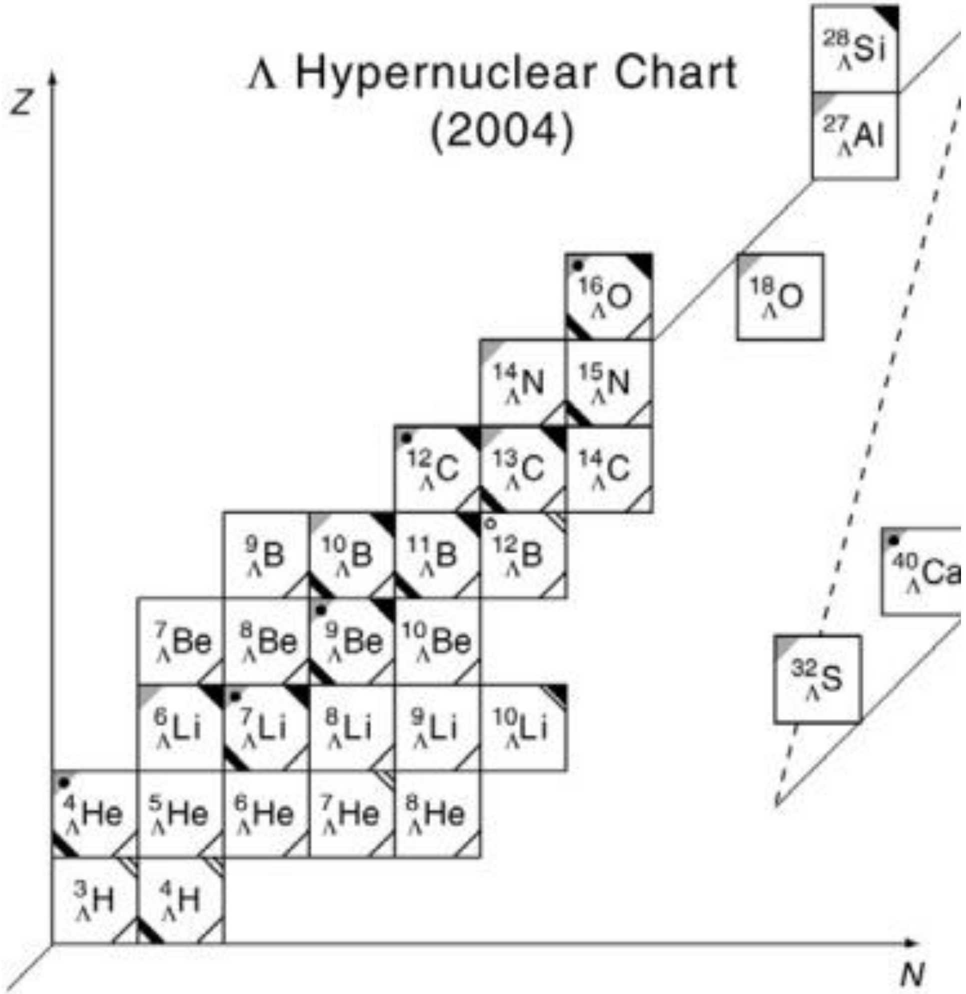


### ●Ξ hypernuclei

Nakazawa, et al., PTEP (2015)
Hayakawa, et al.,PRL (2021)

- $B_\Xi$ from emulsion data
- High resolution $^{12}C(K^-, K^+)^{12}_{\Xi}Be$ experiment planned at J-PARC

etc.

# Situation: Λ hypernuclei

## Binding energy of Λ particle, $B_\Lambda$

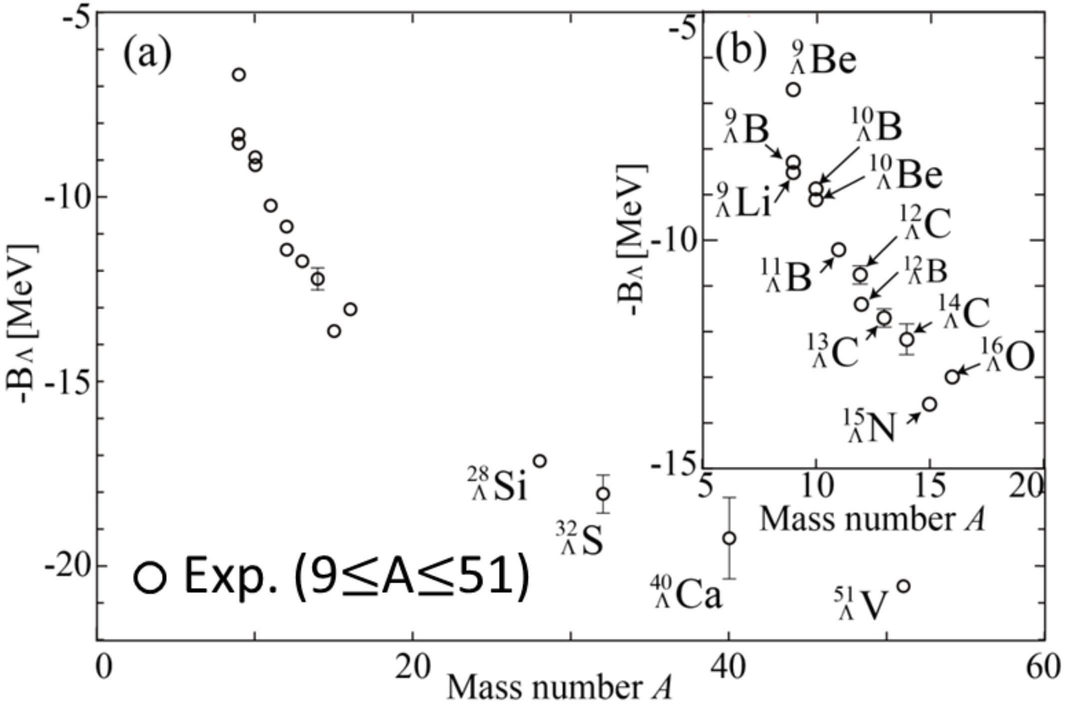


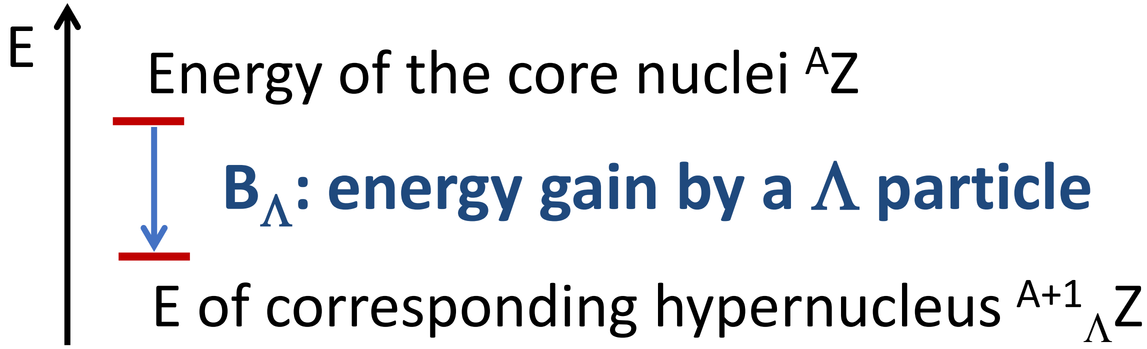


## Level structure of Λ hypernuclei from γ-ray spectroscopy data

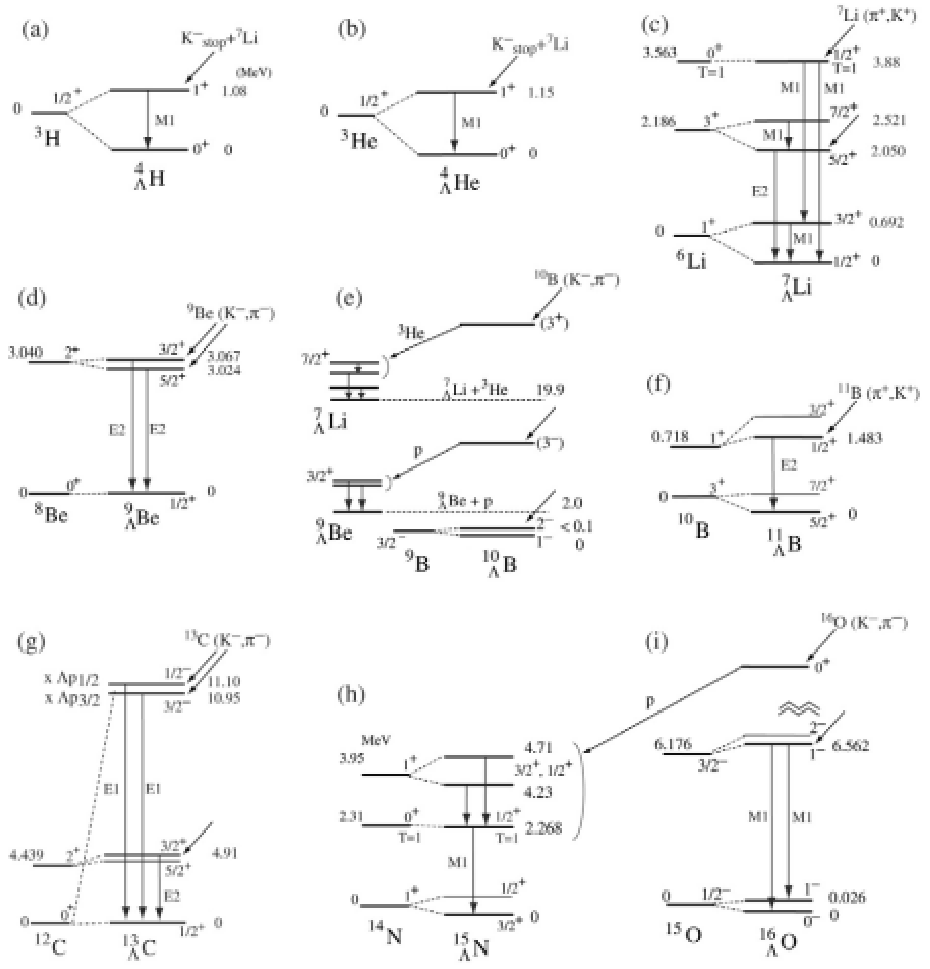


O. Hashimoto and H. Tamura, PPNP **57** (2006), 564.

# Situation: Λ hypernuclei

◆**Future experiments at J-PARC, JLab, *etc*.**

- **Heavier(*sd*-shell) & n-rich hypernuclei can be produced**
- **Various structures will appear**

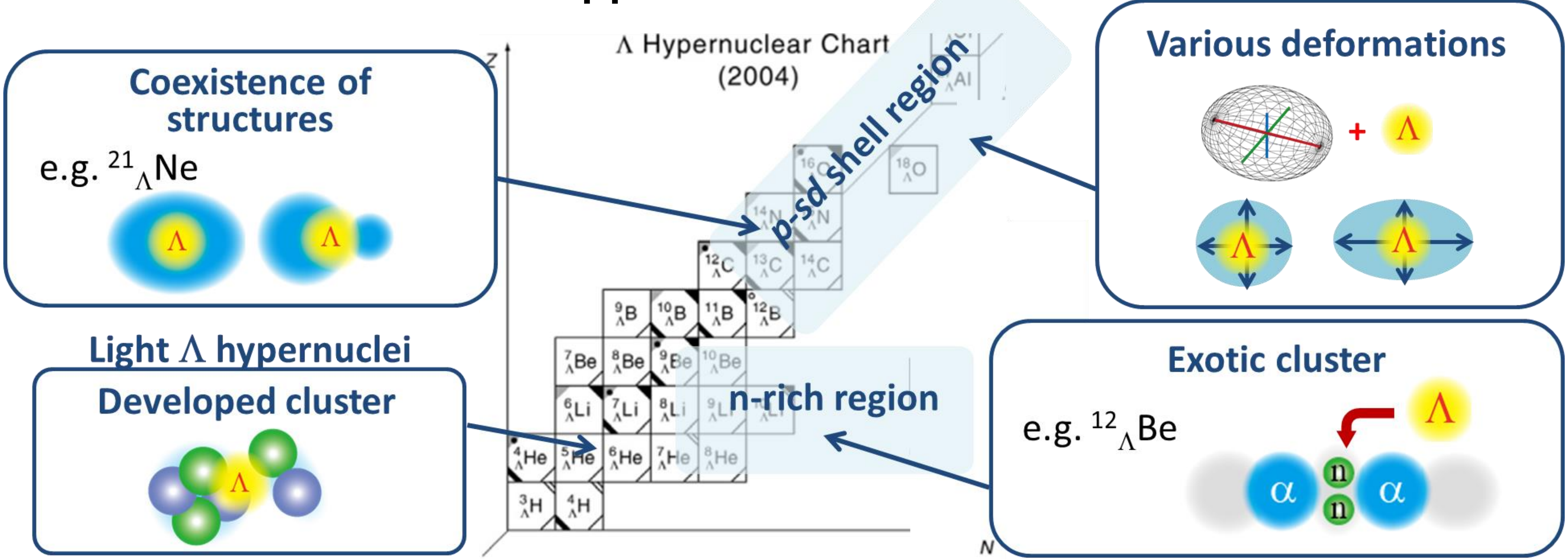


**Structure of hypernuclei can affect the observables of hypernuclei**

# Situation: Ξ hypernuclei

## ◆$B_\Xi$ obtained in $\Xi^- + {}^{14}N$ states

p-state has been identified

- KISO & IBUKI events interpreted as $\Xi^-$ in p-state

K. Nakazawa, et al., PTEP**2015**, 033D02(2015)
S.H. Hayakawa, et al., PRL**126**, 062501(2021)

Deeply bound states have been found
⇒ s-state candidate

- IRRAWADDY & KINKA events

Yoshimoto, et al., arXiv:2103.08793v1

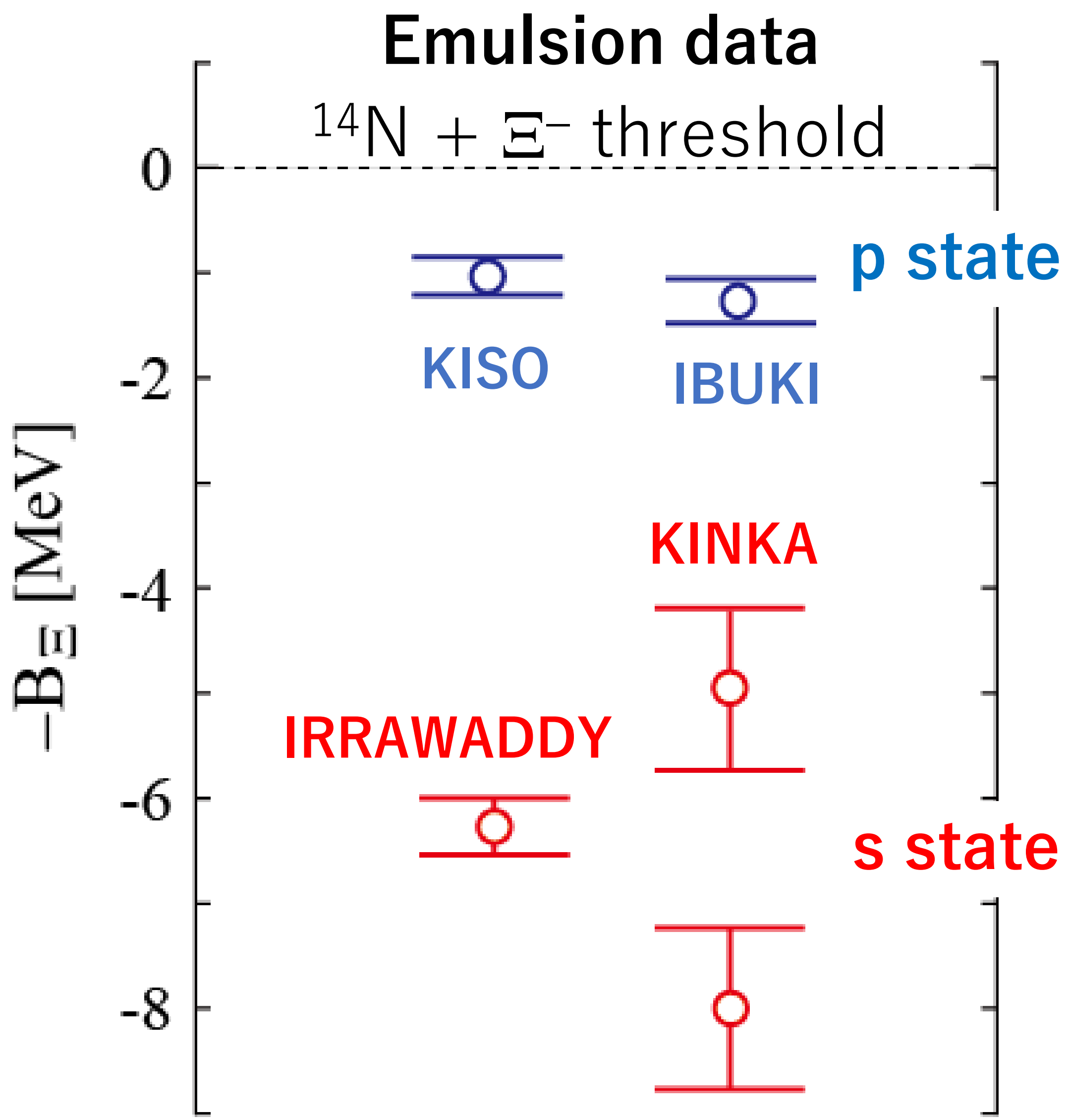

# Theoretical studies on YN interaction

## ◆ΛN

**Interaction models have been developed by comparing with expt.**

- **Few-body calculations**
- **Shell model studies** … etc.

O. Hashimoto and H. Tamura, PPNP **57** (2006), 564
E. Hiyama, and T. Yamada, PPNP**63**, 339(2009)
D.J. Millener, NPA**691** (2001) 93c, Nuclear Phys. A**754** (2005) 48c

### ΛN interaction used in this study

**We use G-matrix interaction derived from Nijmegen potential (YNG)**

- Nijmegen potential: a meson exchange model
- G-matrix calculation takes into account medium effects
- YNG interaction depends on Fermi momentum $k_F$ through nuclear density mainly coming from ΛN-ΣN coupling effects

**$k_F$ can be calculated from density**
e.g. Averaged Density Approximation (ADA)

$$\langle\rho\rangle = \int dr^3 \rho_N(\mathbf{r})\rho_\Lambda(\mathbf{r}) \quad k_F = \left(\frac{3\pi^2\langle\rho\rangle}{2}\right)^{1/3}$$

# Theoretical studies on YN interaction

◆ΞN(S=-2)

ELSEVIER

Check for updates

Available online at www.sciencedirect.com

ScienceDirect

Nuclear Physics A 998 (2020) 121737

NUCLEAR PHYSICS A

www.elsevier.com/locate/nuclphysa

## ΛΛ and NΞ interactions from lattice QCD near the physical point

Kenji Sasaki[a,b,*], Sinya Aoki[a,b,c], Takumi Doi[b,d], Shinya Gongyo[b], Tetsuo Hatsuda[d,b], Yoichi Ikeda[e,b], Takashi Inoue[f,b], Takumi Iritani[b], Noriyoshi Ishii[e,b], Keiko Murano[e,b], Takaya Miyamoto[b]
(HAL QCD Collaboration)

We also use G-matrix interaction derived from HAL QCD ΞN potential to examine it in $\Xi^- + {}^{14}N$

# Topics/Individual problems

## ●Λ hypernuclei

"Mass-dep. of $B_\Lambda$ and importance of describing core deformation"

M. Isaka, Y. Yamamoto, Th.A. Rijken , PRC**94**, 044310(2016)

"Effects of ΛN spin-dependent force on low-lying excitation spectra"

M. Isaka, Y. Yamamoto, T. Motoba, Phys. Rev. C**101**, 024301(2020)

## ●Ξ hypernuclei

"Application of HAL-QCD potential to $\Xi^- + {}^{14}N$ and prediction for ${}^{12}_{\Xi}Be$"

T. Tada, M. Isaka, M. Kimura, Y. Yamamoto

We apply an extended version of antisymmetrized molecular dynamics for hypernuclei (HyperAMD) to Λ and Ξ hypernuclei.

# Theoretical Framework: HyperAMD

M.I., *et al.*, PRC**83**(2011) 044323
M. I., *et al.*, PRC**83**(2011) 054304

## HyperAMD: Antisymmetrized Molecular Dynamics for hypernuclei

### ◆Hamiltonian

$$\hat{H} = \hat{T}_N + \hat{V}_{NN} + \hat{T}_Y + \hat{V}_{YN} - \hat{T}_g$$

**NN : Gogny D1S** (and Volkov No.2 in several Λ hypernuclei)
**YN : G matrix interaction (YNG) derived from**
- **Nijmegen ESC14 (ΛN) for Λ hypernuclei**
- **HAL (ΞN) for Ξ hypernuclei**

### ◆Wave function

- **Nucleon part : Slater determinant**
  Spatial part of s.-p. w.f. is described as Gaussian packets

$$\varphi_N(\vec{r}) = \frac{1}{\sqrt{A!}} \det[\varphi_i(\vec{r}_j)]$$

$$\varphi_i(r) \propto \exp\left[-\sum_{\sigma=x,y,z} \nu_\sigma (r - Z_i)_\sigma^2\right] \chi_i \eta_i$$

$$\chi_i = \alpha_i \chi_\uparrow + \beta_i \chi_\downarrow$$

- **Single-particle w.f. of hyperon:**
  Superposition of Gaussian packets

$$\phi_Y(r) = \sum_m c_m \phi_m(r)$$

$$\varphi_m(r) \propto \exp\left[-\sum_{\sigma=x,y,z} \mu\nu_\sigma (r - z_m)_\sigma^2\right] \chi_m$$

$$\chi_m = a_m \chi_\uparrow + b_m \chi_\downarrow$$

- **Total w.f. :** $\psi(\vec{r}) = \sum_m c_m \phi_m(r_Y) \otimes \frac{1}{\sqrt{A!}} \det[\phi_i(\vec{r}_j)]$

# Theoretical framework: HyperAMD

## ◆Procedure of the calculation

**Variation**

- Imaginary time development method: $\frac{dX_i}{dt} = \frac{\kappa}{\hbar}\frac{\partial H^{\pm}}{\partial X_i^*}$ $\kappa < 0$
- Variational parameters: $X_i = Z_i, z_i, \alpha_i, \beta_i, a_i, b_i, \nu_i, c_i$

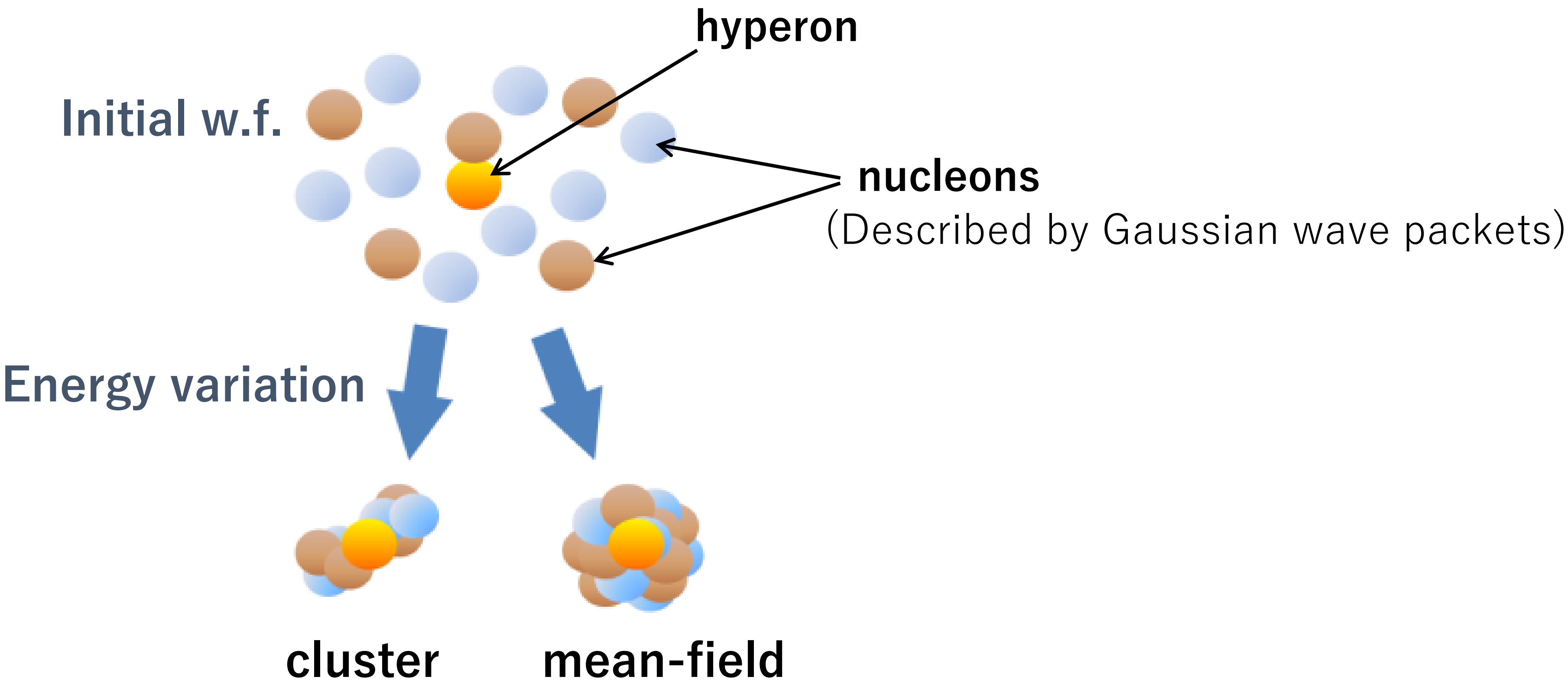

# Theoretical framework: HyperAMD

## ◆Procedure of the calculation

- **Energy variation with constraint on nuclear quadrupole deformation**

Described by $(\beta,\gamma)$

**e.g.) $^{8}$Be**

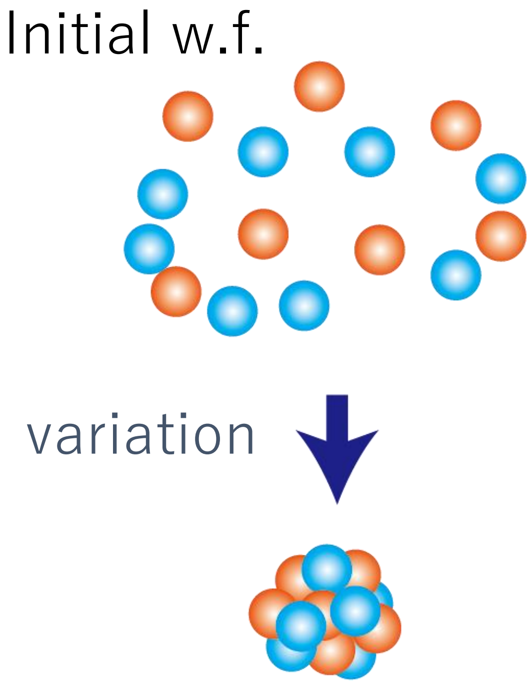


**without constraint on β**

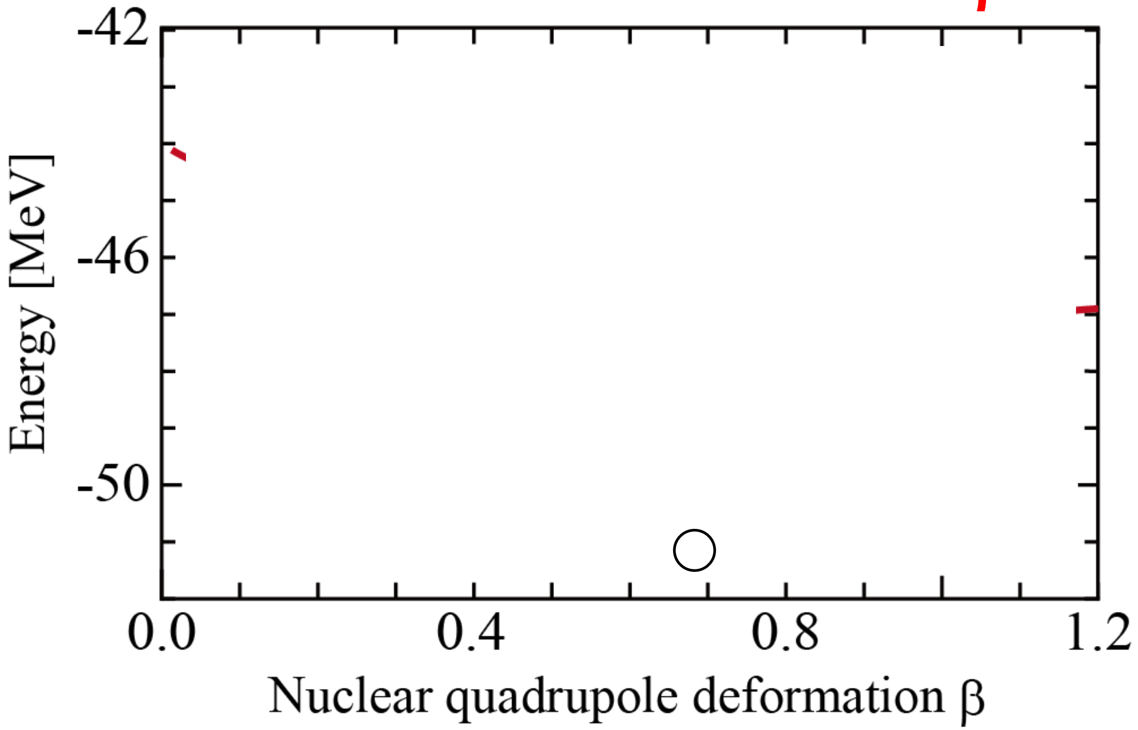

# Theoretical framework: HyperAMD

## ◆Procedure of the calculation

**●Energy variation with constraint on nuclear quadrupole deformation**

Described by $(\beta,\gamma)$

**e.g.) $^{8}$Be**

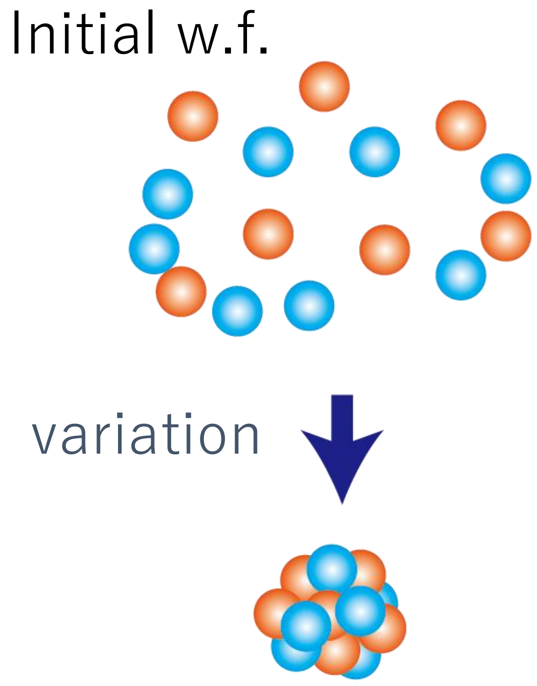


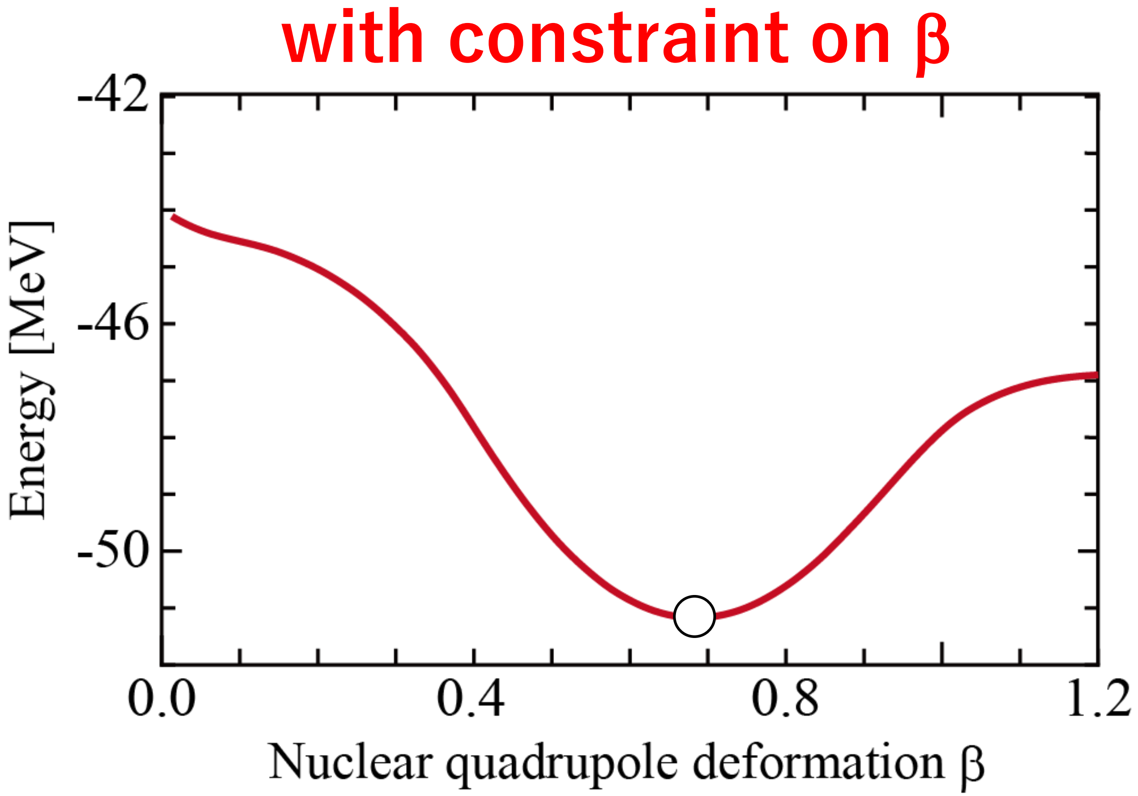

# Theoretical framework: HyperAMD

## ◆Procedure of the calculation

### ●Energy variation with constraint on nuclear quadrupole deformation

e.g.) $^{8}$Be

Initial w.f.

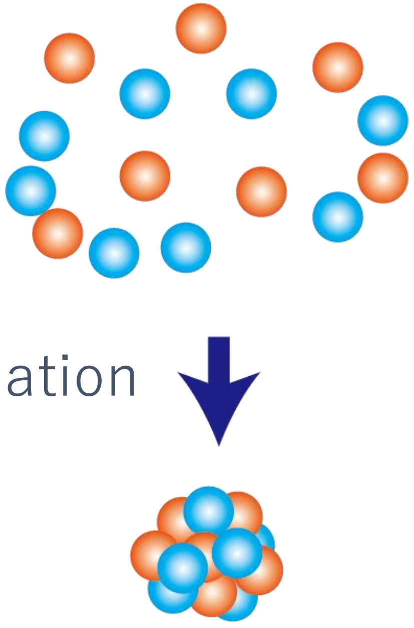


Nuclear density:

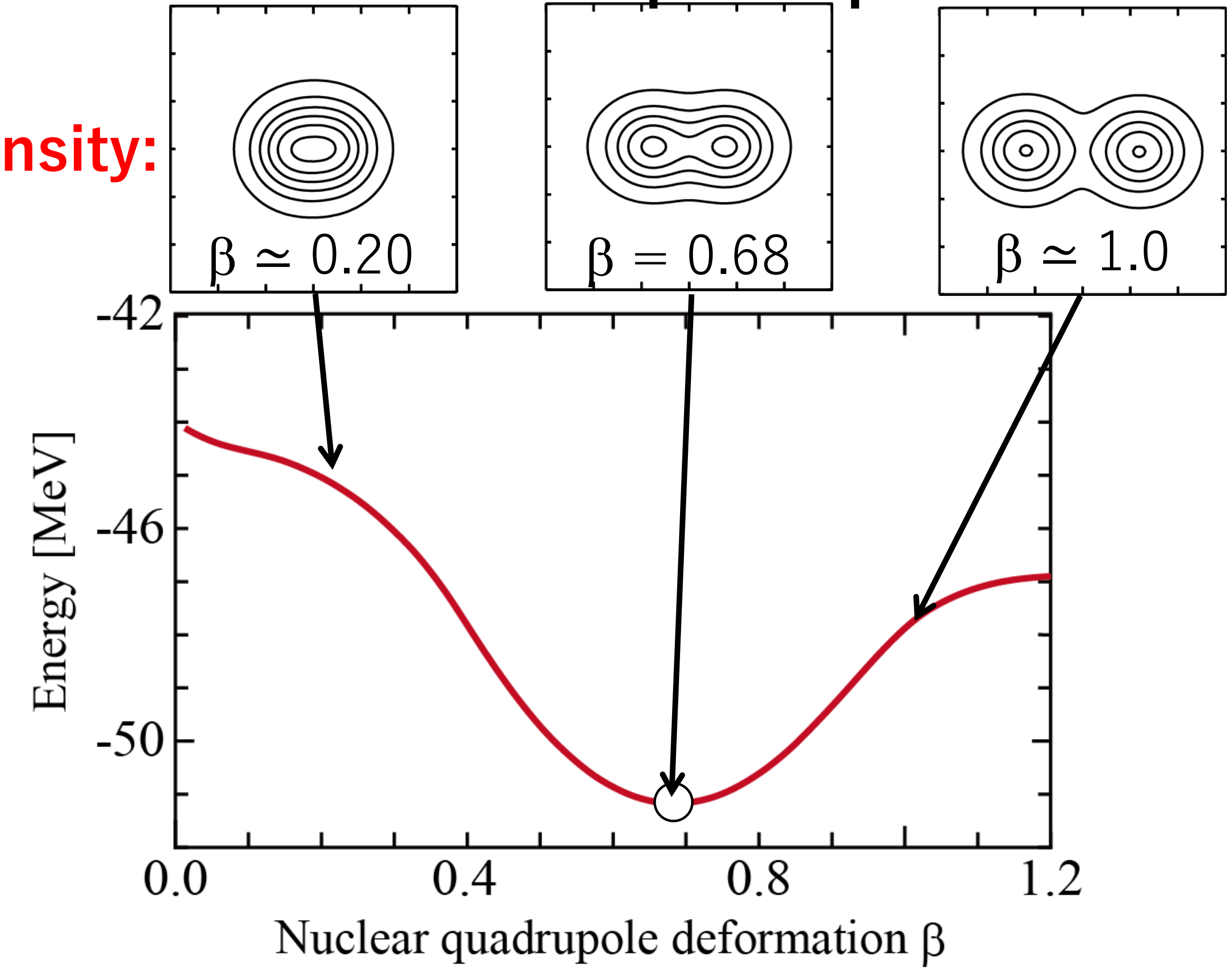

# Actual calculation of HyperAMD

## ◆For hypernuclei

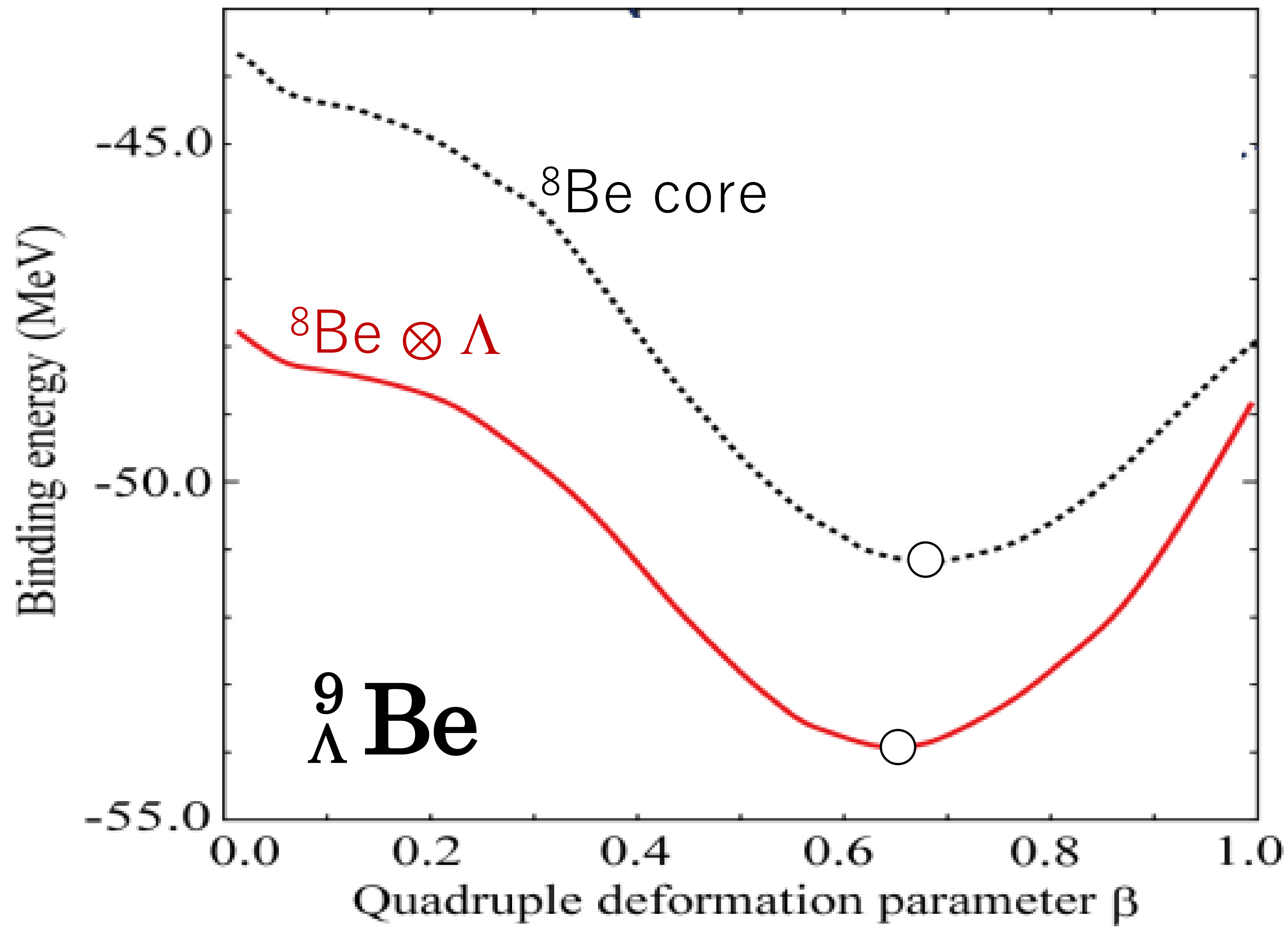

# Theoretical Framework: HyperAMD

## ◆Procedure of the numerical calculation

**Variation**

- Imaginary time development method: $\frac{dX_i}{dt} = \frac{\kappa}{\hbar}\frac{\partial H^{\pm}}{\partial X_i^*}$ $\quad \kappa < 0$
- Variational parameters: $X_i = Z_i, z_i, \alpha_i, \beta_i, a_i, b_i, \nu_i, c_i$

**Angular Momentum Projection**

$$\left|\Phi_K^s; JM\right\rangle = \int d\Omega D_{MK}^{J*}(\Omega) R(\Omega) \left|\Phi^{s+}\right\rangle$$

**Generator Coordinate Method (GCM)**

- Superposition of intrinsic wave functions with different configuration
- Diagonalization of $H_{sK,s'K'}^{J\pm}$ and $N_{sK,s'K'}^{J\pm}$

$$H_{sK,s'K'}^{J\pm} = \left\langle \Phi_K^s; J^{\pm}M \middle| \hat{H} \middle| \Phi_{K'}^{s'}; J^{\pm}M \right\rangle$$

$$N_{sK,s'K'}^{J\pm} = \left\langle \Phi_K^s; J^{\pm}M \middle| \Phi_{K'}^{s'}; J^{\pm}M \right\rangle$$

$$\left|\Psi^{J\pm M}\right\rangle = \sum_{sK} g_{sK} \left|\Phi_K^s; J^{\pm}M\right\rangle$$

# $\Lambda$ hypernuclei

**“Mass-dep. of $B_\Lambda$ and importance of describing core deformation”**

M. Isaka, Y. Yamamoto, Th.A. Rijken , PRC**94**, 044310(2016)

**“Effects of $\Lambda$N spin-dependent force on low-lying excitation spectra”**

M. Isaka, Y. Yamamoto, T. Motoba, Phys. Rev. C**101**, 024301(2020)

# Results: $B_\Lambda$ as a function of mass number *A*

- **HyperAMD calc. with YNG ΛN interaction for $9 \le A \le 59$ Λ hypernuclei**

Averaged Density Approximation (ADA)

$$\langle\rho\rangle = \int dr^3 \rho_N(\mathbf{r})\rho_\Lambda(\mathbf{r}) \qquad k_F = (1+\alpha)\left(\frac{3\pi^2\langle\rho\rangle}{2}\right)^{1/3}$$

Small parameter α is chosen to reproduce $B_\Lambda$ of $^{16}_{\Lambda}$O (α = -0.009)

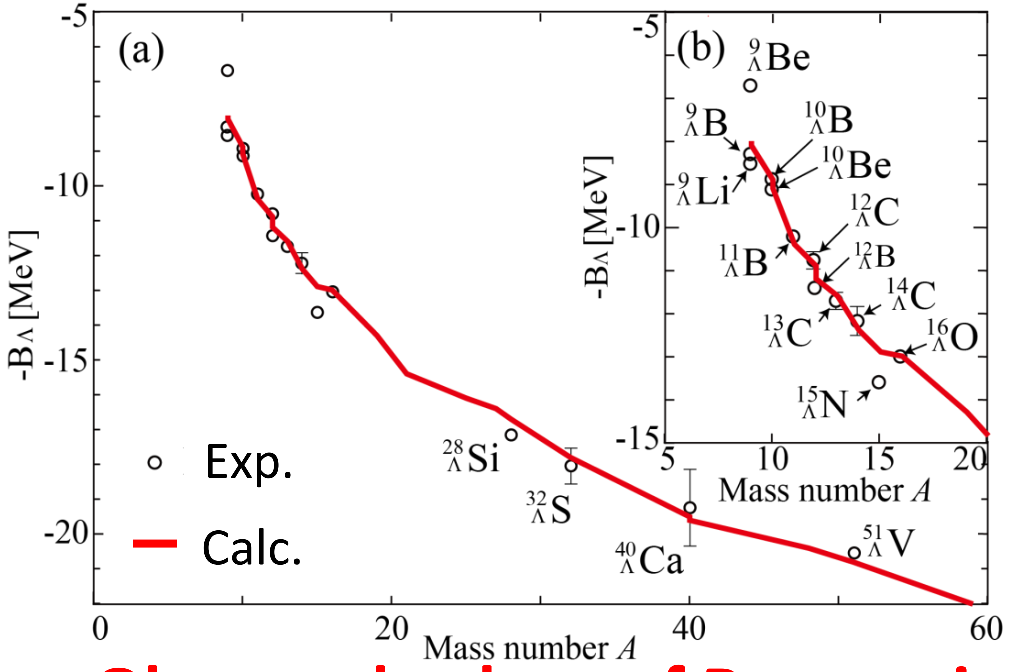


| | $\beta$ | $\gamma$ | $\langle\rho\rangle$ | $k_F$ | $-B_\Lambda^{calc}$ | $-B_\Lambda^{exp}$ |
|---|---|---|---|---|---|---|
| $^{9}_{\Lambda}$Li | 0.50 | 2° | 0.072 | 1.01 | −8.1 | −8.50 ± 0.12 |
| $^{9}_{\Lambda}$Be | 0.87 | 1° | 0.060 | 0.95 | −8.0 | −6.71 ± 0.04 |
| $^{9}_{\Lambda}$B | 0.45 | 2° | 0.072 | 1.01 | −8.1 | −8.29 ± 0.18 |
| $^{10}_{\Lambda}$Be | 0.57 | 1° | 0.077 | 1.04 | −8.9 | −9.11 ± 0.22 |
| | | | | | | −8.55 ± 0.18 |
| $^{10}_{\Lambda}$B | 0.58 | 1° | 0.075 | 1.03 | −9.1 | −8.89 ± 0.12 |
| $^{11}_{\Lambda}$B | 0.50 | 29° | 0.081 | 1.05 | −10.4 | −10.24 ± 0.05 |
| $^{12}_{\Lambda}$B | 0.39 | 48° | 0.083 | 1.06 | −11.2 | −11.37 ± 0.06 |
| | | | | | | −11.38 ± 0.02 |
| $^{12}_{\Lambda}$C | 0.41 | 34° | 0.086 | 1.07 | −10.9 | −10.76 ± 0.19 |
| $^{13}_{\Lambda}$C | 0.45 | 60° | 0.090 | 1.09 | −11.6 | −11.69 ± 0.19 |
| $^{14}_{\Lambda}$C | 0.45 | 31° | 0.093 | 1.10 | −12.4 | −12.17 ± 0.33 |
| $^{15}_{\Lambda}$N | 0.28 | 60° | 0.098 | 1.12 | −12.9 | −13.59 ± 0.15 |
| $^{16}_{\Lambda}$O | 0.02 | – | 0.105 | 1.15 | −13.0 | −12.96 ± 0.05 |
| $^{19}_{\Lambda}$O | 0.30 | 3° | 0.110 | 1.17 | −14.3 | – |
| $^{21}_{\Lambda}$Ne | 0.46 | 0° | 0.106 | 1.15 | −15.4 | – |
| $^{25}_{\Lambda}$Mg | 0.478 | 21° | 0.116 | 1.19 | −16.1 | – |
| $^{27}_{\Lambda}$Mg | 0.36 | 36° | 0.125 | 1.22 | −16.4 | – |
| $^{28}_{\Lambda}$Si | 0.32 | 53° | 0.125 | 1.22 | −16.7 | −17.1 ± 0.02 |
| $^{32}_{\Lambda}$S | 0.28 | 0° | 0.130 | 1.23 | −17.8 | −18.0 ± 0.5 |
| $^{40}_{\Lambda}$K | 0.01 | – | 0.136 | 1.25 | −19.6 | – |
| $^{40}_{\Lambda}$Ca | 0.03 | – | 0.136 | 1.25 | −19.5 | −19.24 ± 1.1 |
| $^{41}_{\Lambda}$Ca | 0.13 | 12° | 0.136 | 1.25 | −19.7 | – |
| $^{48}_{\Lambda}$K | 0.01 | – | 0.141 | 1.27 | −20.4 | – |
| $^{51}_{\Lambda}$V | 0.18 | 2° | 0.151 | 1.30 | −20.8 | −20.51 ± 0.13 |
| $^{59}_{\Lambda}$Fe | 0.26 | 23° | 0.142 | 1.27 | −22.0 | – |

**Observed values of $B_\Lambda$ are nicely reproduced in wide mass regions**

# What is essential to reproduce $B_\Lambda$?

**"Full calc." vs. "Spherical calc."**

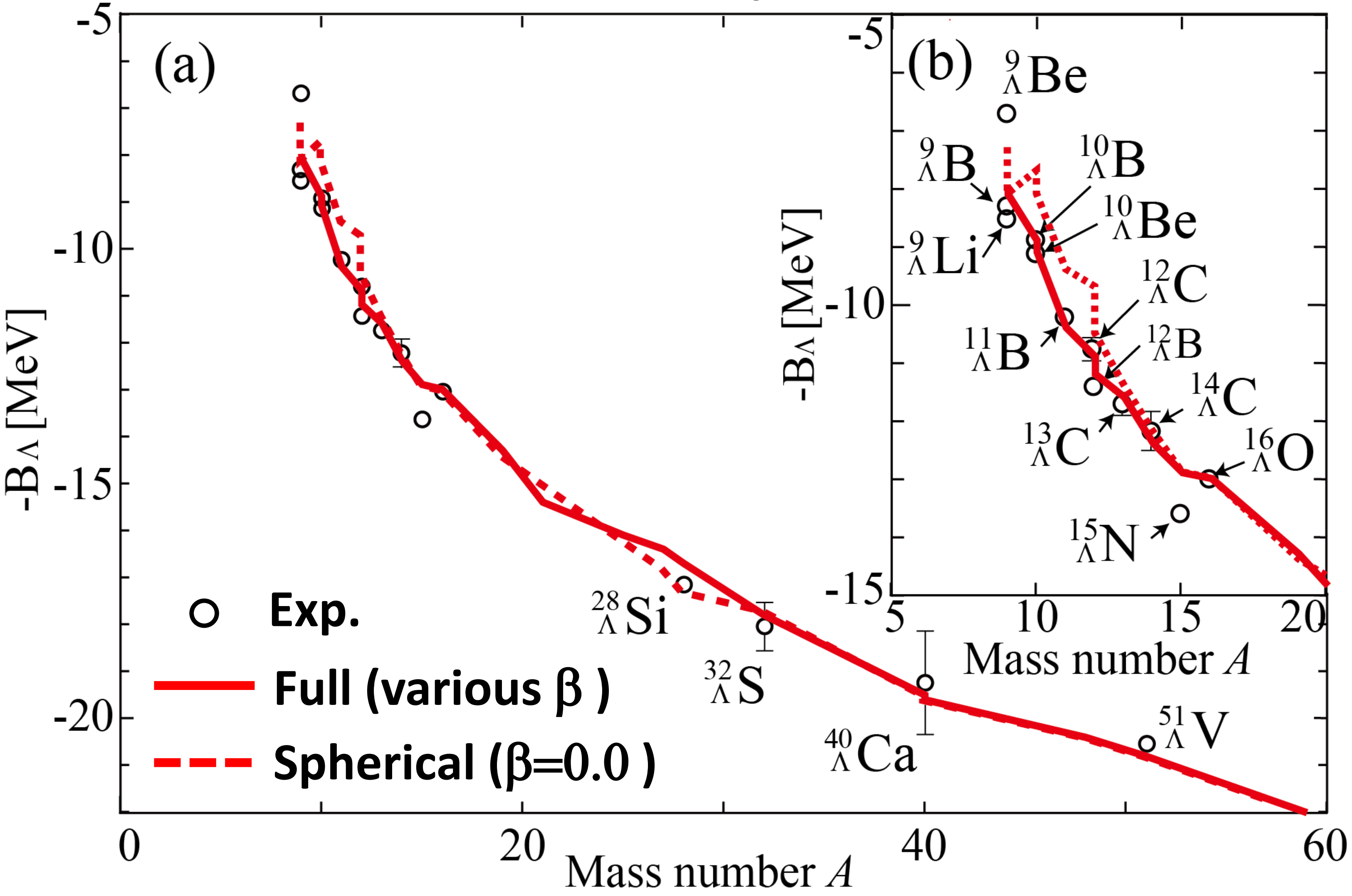


**"Spherical calculation"**
**using intrinsic state with β = 0 only**

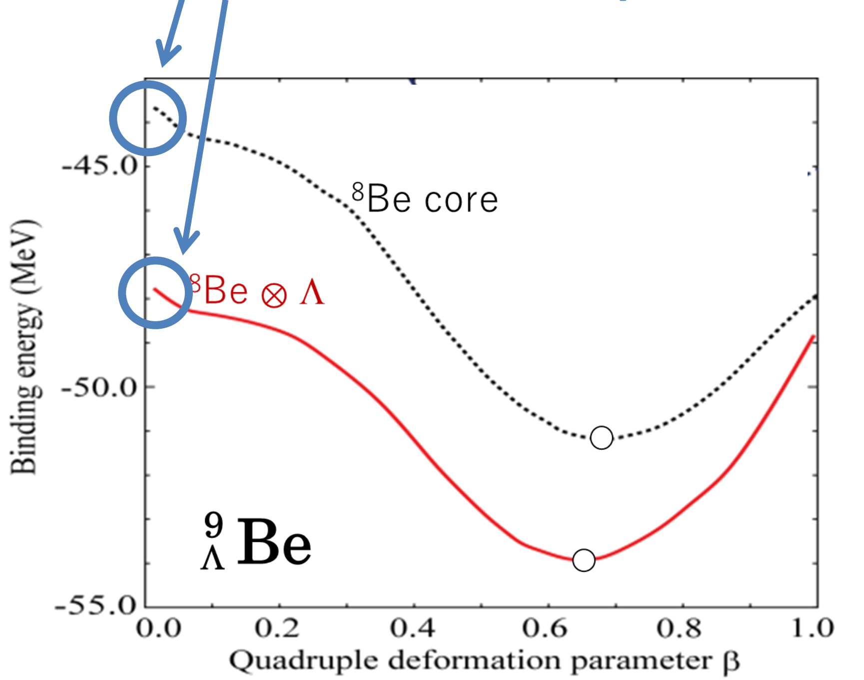


**"Full calculation"**
**using all intrinsic wave functions on the energy surface**

**$B_\Lambda$ values are reproduced by taken into account nuclear deformation**

# What is essential to reproduce $B_\Lambda$?

## ◆Description of core deformation

**Example: $^{11}$B**

More sophisticated treatment: GCM calculation on (β, γ) plane

Comparison of B(E2) with observed data in $^{11}$B

AMD with β-γ const.:
we follow Suhara and Kanada-En'yo, PTP**123**,303(2010)

Present calc. (AMD)

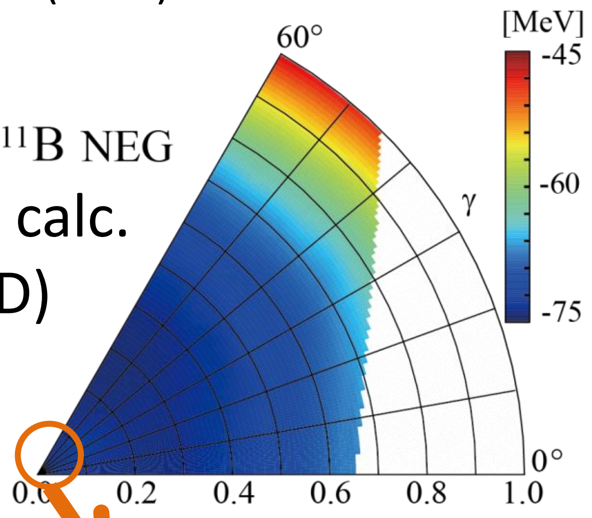


+ Λ

**$^{12}_{\Lambda}$B (Spherical)**

**$B_\Lambda$ = 9.7 MeV**

**($k_F$ = 1.15 fm$^{-1}$)**

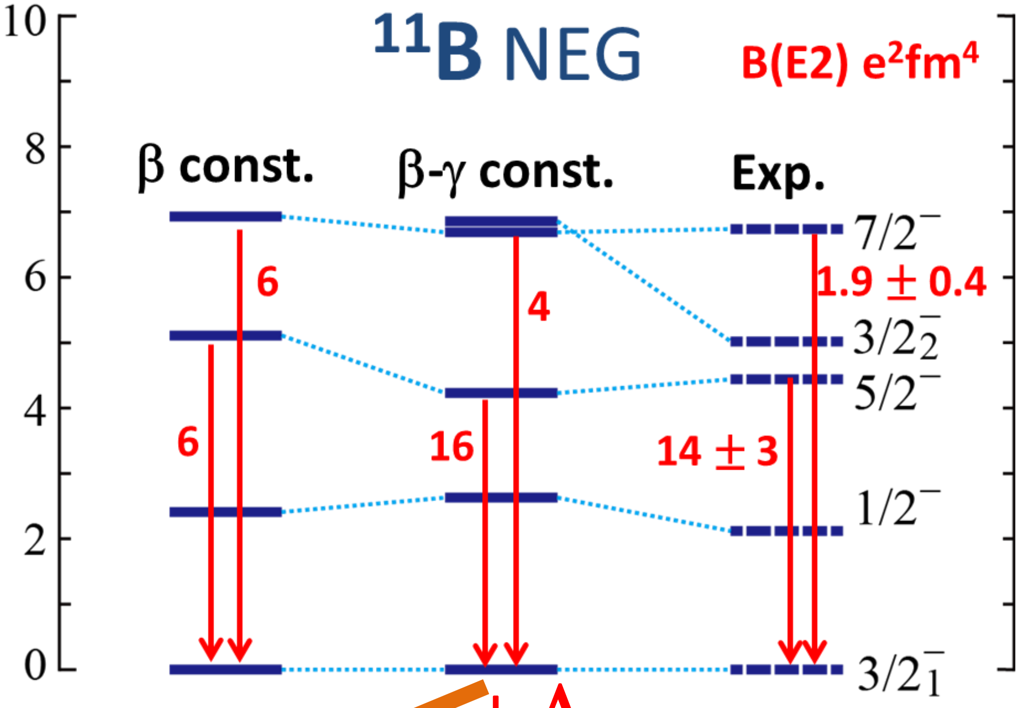


+ Λ

**$^{12}_{\Lambda}$B (β-γ)**

**$B_\Lambda$ = 11.2 MeV**

**($k_F$ = 1.06 fm$^{-1}$)**

**$^{12}_{\Lambda}$B (EXP)**

**$B_\Lambda$ = 11.4 ±0.02 MeV**

# $\Lambda$ hypernuclei

**"Mass-dep. of $B_\Lambda$ and importance of describing core deformation"**

M. Isaka, Y. Yamamoto, Th.A. Rijken , PRC**94**, 044310(2016)

**"Effects of $\Lambda$N spin-dependent force on low-lying excitation spectra"**

M. Isaka, Y. Yamamoto, T. Motoba, Phys. Rev. C**101**, 024301(2020)

# Results: $B_\Lambda$ as a function of mass number *A*

- **HyperAMD calc. with YNG ΛN interaction for $9 \le A \le 59$ Λ hypernuclei**

Averaged Density Approximation (ADA)

$$\langle\rho\rangle = \int dr^3 \rho_N(\mathbf{r})\rho_\Lambda(\mathbf{r}) \quad k_F = (1+\alpha)\left(\frac{3\pi^2\langle\rho\rangle}{2}\right)^{1/3}$$

Small parameter α is chosen to reproduce $B_\Lambda$ of $^{16}_{\Lambda}$O (α = -0.009)

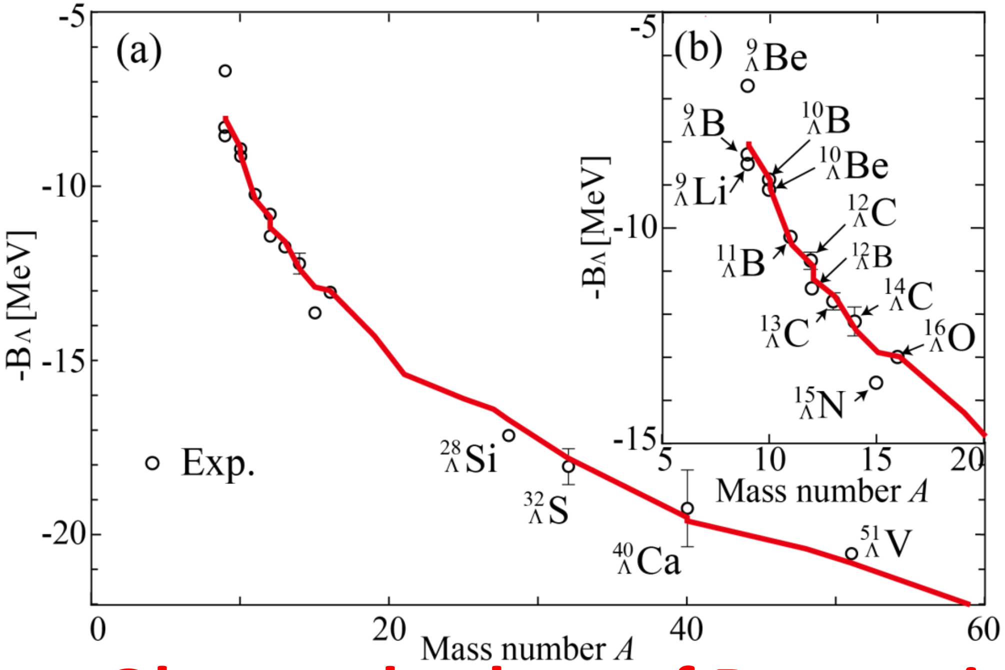


| | $\beta$ | $\gamma$ | $\langle\rho\rangle$ | $k_F$ | $-B_\Lambda^{calc}$ | $-B_\Lambda^{exp}$ |
|---|---|---|---|---|---|---|
| $^{9}_{\Lambda}$Li | 0.50 | 2° | 0.072 | 1.01 | −8.1 | −8.50 ± 0.12 |
| $^{9}_{\Lambda}$Be | 0.87 | 1° | 0.060 | 0.95 | −8.0 | −6.71 ± 0.04 |
| $^{9}_{\Lambda}$B | 0.45 | 2° | 0.072 | 1.01 | −8.1 | −8.29 ± 0.18 |
| $^{10}_{\Lambda}$Be | 0.57 | 1° | 0.077 | 1.04 | −8.9 | −9.11 ± 0.22 |
| | | | | | | −8.55 ± 0.18 |
| $^{10}_{\Lambda}$B | 0.58 | 1° | 0.075 | 1.03 | −9.1 | −8.89 ± 0.12 |
| $^{11}_{\Lambda}$B | 0.50 | 29° | 0.081 | 1.05 | −10.4 | −10.24 ± 0.05 |
| $^{12}_{\Lambda}$B | 0.39 | 48° | 0.083 | 1.06 | −11.2 | −11.37 ± 0.06 |
| | | | | | | −11.38 ± 0.02 |
| $^{12}_{\Lambda}$C | 0.41 | 34° | 0.086 | 1.07 | −10.9 | −10.76 ± 0.19 |
| $^{13}_{\Lambda}$C | 0.45 | 60° | 0.090 | 1.09 | −11.6 | −11.69 ± 0.19 |
| $^{14}_{\Lambda}$C | 0.45 | 31° | 0.093 | 1.10 | −12.4 | −12.17 ± 0.33 |
| $^{15}_{\Lambda}$N | 0.28 | 60° | 0.098 | 1.12 | −12.9 | −13.59 ± 0.15 |
| $^{16}_{\Lambda}$O | 0.02 | – | 0.105 | 1.15 | −13.0 | −12.96 ± 0.05 |
| $^{19}_{\Lambda}$O | 0.30 | 3° | 0.110 | 1.17 | −14.3 | – |
| $^{21}_{\Lambda}$Ne | 0.46 | 0° | 0.106 | 1.15 | −15.4 | – |
| $^{25}_{\Lambda}$Mg | 0.478 | 21° | 0.116 | 1.19 | −16.1 | – |
| $^{27}_{\Lambda}$Mg | 0.36 | 36° | 0.125 | 1.22 | −16.4 | – |
| $^{28}_{\Lambda}$Si | 0.32 | 53° | 0.125 | 1.22 | −16.7 | −17.1 ± 0.02 |
| $^{32}_{\Lambda}$S | 0.28 | 0° | 0.130 | 1.23 | −17.8 | −18.0 ± 0.5 |
| $^{40}_{\Lambda}$K | 0.01 | – | 0.136 | 1.25 | −19.6 | – |
| $^{40}_{\Lambda}$Ca | 0.03 | – | 0.136 | 1.25 | −19.5 | −19.24 ± 1.1 |
| $^{41}_{\Lambda}$Ca | 0.13 | 12° | 0.136 | 1.25 | −19.7 | – |
| $^{48}_{\Lambda}$K | 0.01 | – | 0.141 | 1.27 | −20.4 | – |
| $^{51}_{\Lambda}$V | 0.18 | 2° | 0.151 | 1.30 | −20.8 | −20.51 ± 0.13 |
| $^{59}_{\Lambda}$Fe | 0.26 | 23° | 0.142 | 1.27 | −22.0 | – |

**Observed values of $B_\Lambda$ are nicely reproduced in wide mass regions**

# Results: $B_\Lambda$ as a function of mass number *A*

| | $\langle\rho\rangle$ | $k_F$ | Based on ESC12 [17] | | | | Based on ESC14 | | | | Expt. | |
|---|---|---|---|---|---|---|---|---|---|---|---|---|
| | | | $V_{BB}$ only | | w/ MBE | | $V_{BB}$ only | | w/ MBE | | $J^\pi$ | $-B_\Lambda^{\rm exp}$ |
| | | | $J^\pi$ | $-B_\Lambda$ | $J^\pi$ | $-B_\Lambda$ | $J^\pi$ | $-B_\Lambda$ | $J^\pi$ | $-B_\Lambda$ | | |
| $^{9}_{\Lambda}$Li(∗) | 0.072 | 1.02 | $5/2^+$ | −7.9 | $5/2^+$ | −8.1 | $5/2^+$ | −7.6 | $5/2^+$ | −8.1 | | $-8.50 \pm 0.12$ [34] |
| $^{9}_{\Lambda}$Be | 0.060 | 0.96 | $1/2^+$ | −7.9 | $1/2^+$ | −8.1 | $1/2^+$ | −7.7 | $1/2^+$ | −8.1 | $1/2^+$ | $-6.71 \pm 0.04$ [28] |
| $^{9}_{\Lambda}$B(∗) | 0.072 | 1.02 | $5/2^+$ | −8.0 | $5/2^+$ | −8.2 | $5/2^+$ | −7.7 | $5/2^+$ | −8.2 | | $-8.29 \pm 0.18$ [34] |
| $^{10}_{\Lambda}$Be(∗) | 0.077 | 1.04 | $2^-$ | −8.7 | $2^-$ | −9.0 | $2^-$ | −8.6 | $2^-$ | −9.0 | | $-9.11 \pm 0.22$ [31], $-8.55 \pm 0.18$ [37] |
| $^{10}_{\Lambda}$B(∗) | 0.075 | 1.04 | $2^-$ | −8.9 | $2^-$ | −9.2 | $2^-$ | −8.7 | $2^-$ | −9.1 | $1^-$ [38,39] | $-8.89 \pm 0.12$ [28] |
| $^{11}_{\Lambda}$B(∗) | 0.081 | 1.05 | $7/2^+$ | −9.8 | $7/2^+$ | −10.1 | $7/2^+$ | −9.7 | $7/2^+$ | −10.0 | $5/2^+$ [40] | $-10.24 \pm 0.05$ [28] |
| $^{12}_{\Lambda}$B(∗) | 0.083 | 1.07 | $2^-$ | −11.0 | $2^-$ | −11.3 | $2^-$ | −11.0 | $2^-$ | −11.3 | $1^-$ [41–43] | $-11.37 \pm 0.06$ [28], $-11.38 \pm 0.02$ [36] |
| $^{12}_{\Lambda}$C(∗) | 0.086 | 1.08 | $2^-$ | −10.7 | $2^-$ | −11.0 | $2^-$ | −10.8 | $2^-$ | −11.0 | $1^-$ [44] | $-10.76 \pm 0.19$ [34] |
| $^{13}_{\Lambda}$C(∗) | 0.090 | 1.10 | $1/2^+$ | −11.3 | $1/2^+$ | −11.6 | $1/2^+$ | −11.5 | $1/2^+$ | −11.7 | $1/2^+$ | $-11.69 \pm 0.19$ [31] |
| $^{14}_{\Lambda}$C(∗) | 0.093 | 1.11 | $0^-$ | −12.4 | $0^-$ | −12.5 | $0^-$ | −12.4 | $0^-$ | −12.5 | | $-12.17 \pm 0.33$ [34] |
| $^{15}_{\Lambda}$N | 0.098 | 1.13 | $1/2^+$ | −12.6 | $1/2^+$ | −12.9 | $1/2^+$ | −12.9 | $1/2^+$ | −12.9 | $3/2^+$ [38] | $-13.59 \pm 0.15$ [28] |
| $^{16}_{\Lambda}$O(∗) | 0.105 | 1.16 | $0^-$ | −12.7 | $0^-$ | −13.0 | $1^-$ | −13.3 | $1^-$ | −13.0 | $0^-$ [45] | $-12.96 \pm 0.05$ [32]† |

- **Mass-dependence of $B_\Lambda$ is reproduced with describing core deformation**
- **However, ground-state spin is inconsistent with exp. in several hypernuclei**

# Inconsistent ground-state spin in our previous work

- **Found in $^{10}_{\Lambda}$B, $^{11}_{\Lambda}$B, $^{12}_{\Lambda}$B, $^{12}_{\Lambda}$C, $^{15}_{\Lambda}$N, and $^{16}_{\Lambda}$O with spin-doublet ground states, where the core nuclei have non-zero spin ground states**

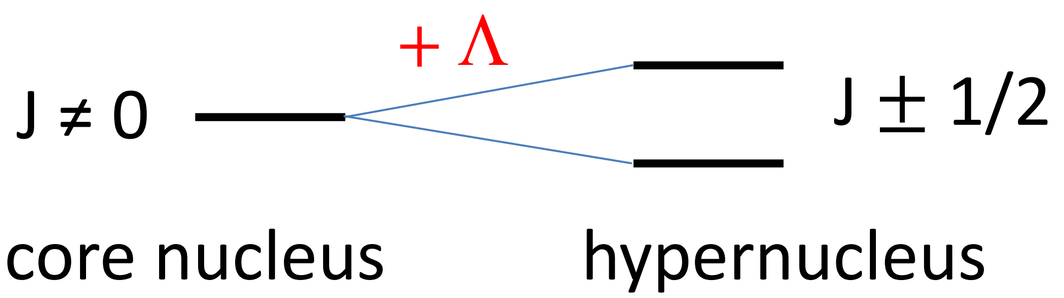


Coupling of Λ generates ground state doublets

- **Inconsistency originates in different ordering of doublet partner**
- **Ordering is expected to be determined by ΛN spin-dependent force**

ΛN spin-spin force: $V^{\mathrm{central}}_{\Lambda N} = V^{\mathrm{Even}} + (\sigma\cdot\sigma)V^{\mathrm{Even}}_{\sigma} + V^{\mathrm{Odd}} + (\sigma\cdot\sigma)V^{\mathrm{Odd}}_{\sigma}$

ΛN Spin-orbit (LS) force: $V^{\mathrm{LS}}_{\Lambda N} = \mathbf{L}\cdot(\mathbf{s}_{\Lambda} + \mathbf{s}_{N})V^{\mathrm{SLS}} + \mathbf{L}\cdot(\mathbf{s}_{\Lambda} - \mathbf{s}_{N})V^{\mathrm{ALS}}$

Aim of this work

○ We reveal effects of ΛN spin-dependent (spin-spin & spin-orbit) forces

# Tuning of ΛN spin-dependent force

**Information on ΛN spin-dep. force can be obtained by doublet energies in light Λ hypernuclei**

E. Hiyama, and T. Yamada, PPNP**63**, 339(2009), and references therein

e.g.) spin-spin force in ΛN central force

$$V_{\Lambda N}^{\mathrm{central}} = V^{\mathrm{Even}} + (\sigma\cdot\sigma)V_{\sigma}^{\mathrm{Even}} + V^{\mathrm{Odd}} + (\sigma\cdot\sigma)V_{\sigma}^{\mathrm{Odd}}$$

Example: ${}^{4}_{\Lambda}$H

p n n 0s   Λ 0s

${}^{3}\mathrm{H}(J^{\pi} = 1/2^{+}) \otimes \Lambda(S = 1/2)$

- Even state force dominated
- Doublet by spin-spin force

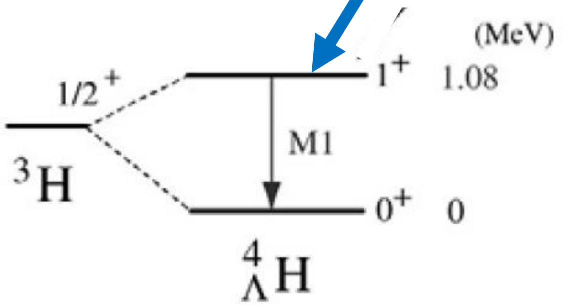


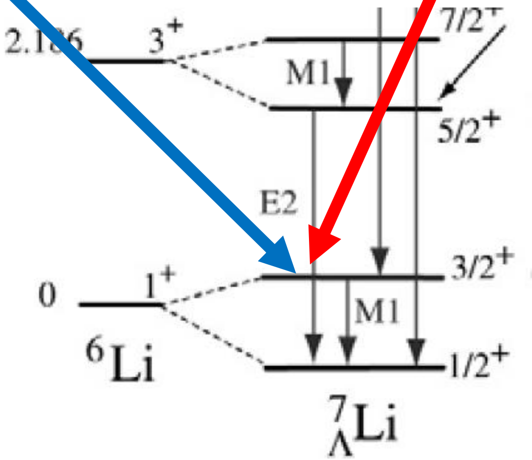


Core nucleus ${}^{6}$Li

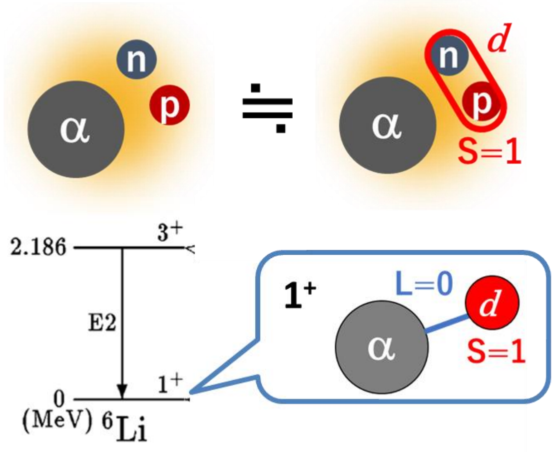


**In this study, we tune ΛN spin-dependent force following the above**

Figures taken from O. Hashimoto and H. Tamura, PPNP**57** (2006), 564

# Results: Tuning of spin-dep. ΛN forces in HyperAMD

Central: $V_{\Lambda N}^{central} = V^{Even} + (\sigma\cdot\sigma)\mathbf{V_{\sigma}^{Even}} + V^{Odd} + (\sigma\cdot\sigma)\mathbf{V_{\sigma}^{Odd}}$

LS: $V_{\Lambda N}^{LS} = \mathbf{L}\cdot(\mathbf{s}_\Lambda + \mathbf{s}_N)V^{SLS} + \mathbf{L}\cdot(\mathbf{s}_\Lambda - \mathbf{s}_N)V^{ALS}$

- **Adding correction terms $\Delta V_\sigma^E$, $\Delta V_\sigma^O$ to $\sigma\cdot\sigma$ parts**
- **LS is tuned using the (3/2⁺, 5/2⁺) data of $^{9}_{\Lambda}$Be**

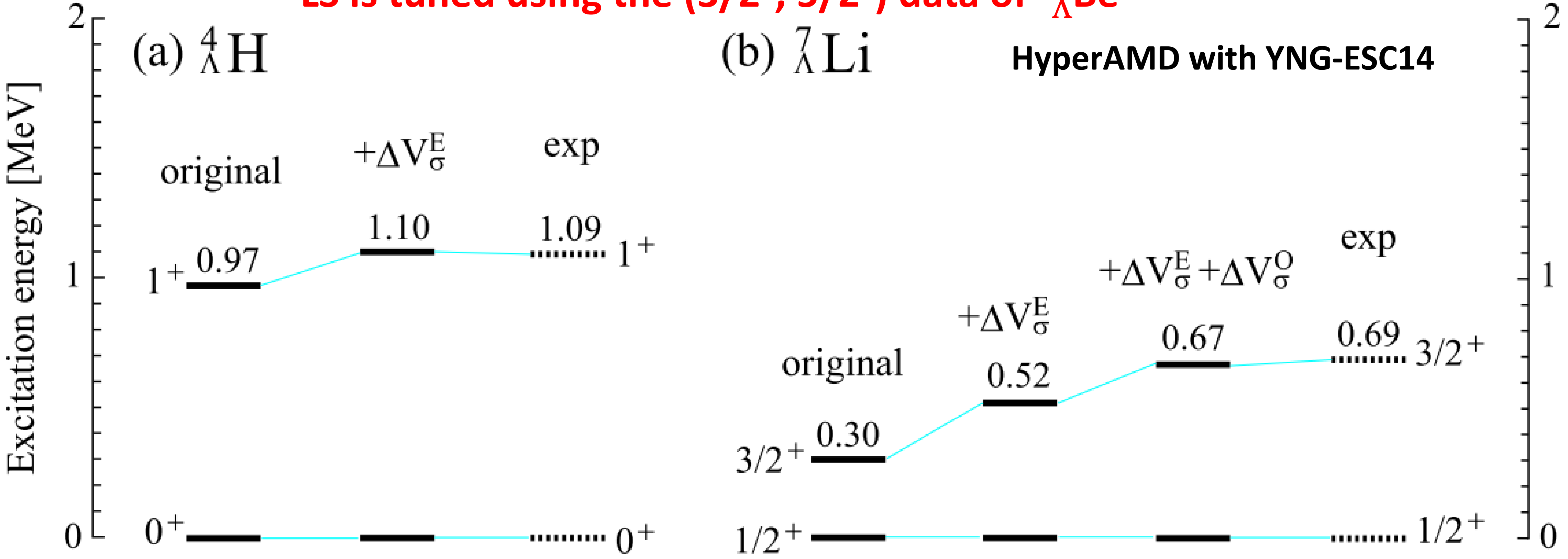


*We apply the ΛN interaction tuned here to p-shell hypernuclei*

# Results: p-shell Λ hypernuclei

## ◆$^{7}_{\Lambda}$Li: a well-known p-shell hypernucleus

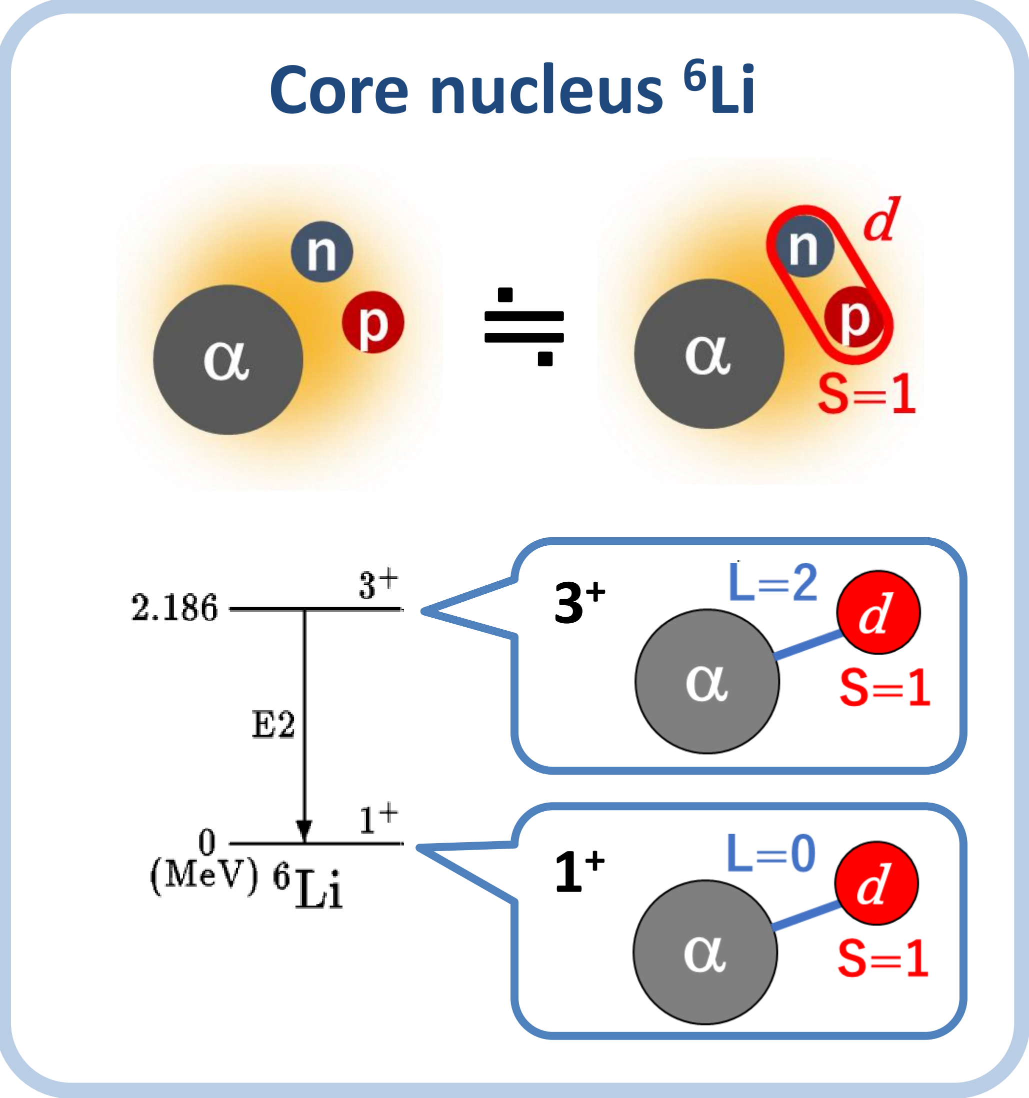


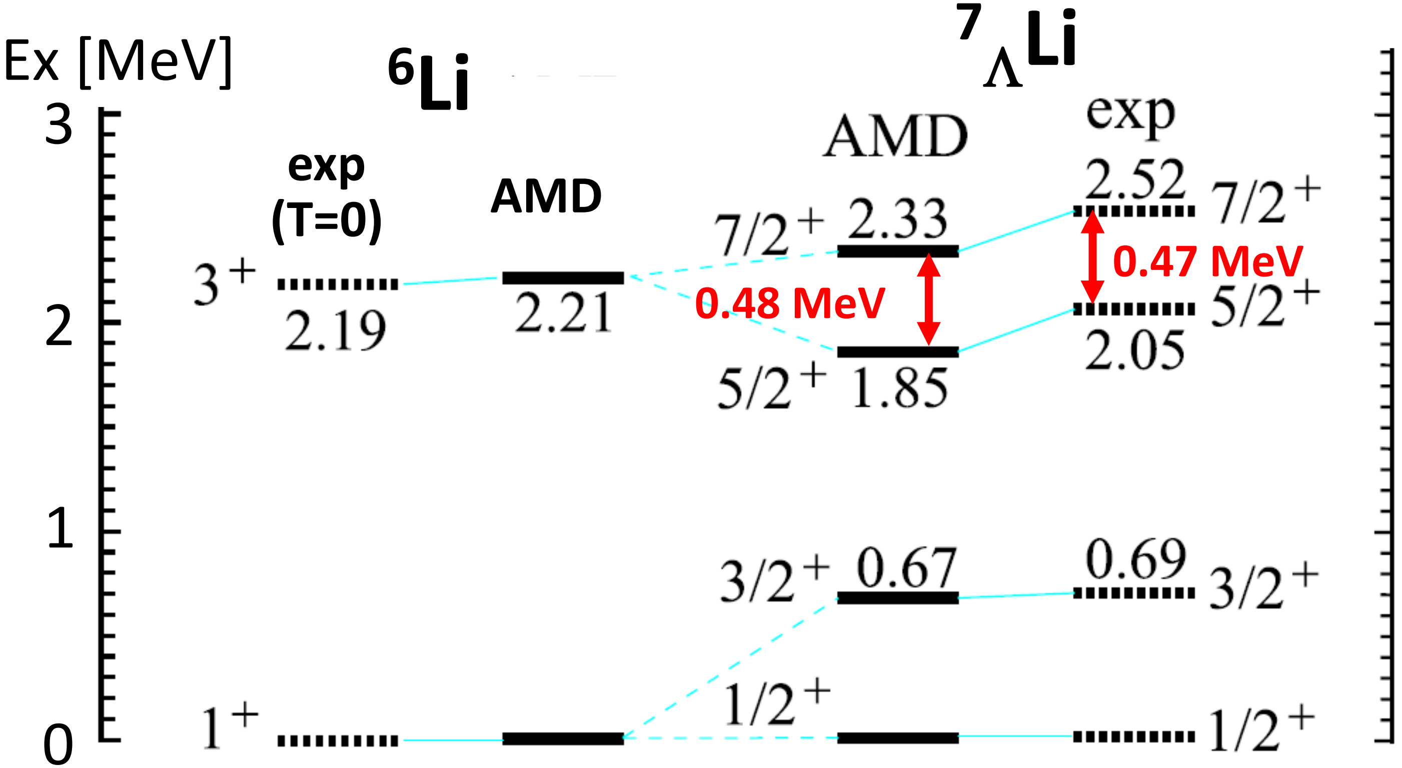


- Ground-state doublet ($1/2^+$,$3/2^+$) is used to tune ΛN spin-spin force, where almost no LS contribution
- Spin-dependent central and LS forces contribute to ($5/2^+$,$7/2^+$) doublet

→ **Reproduced by tuned ΛN force**

# Results: p-shell Λ hypernuclei

**Tuned ΛN force systematically reproduces ground state spin & doublet spacing**

HyperAMD with YNG-ESC14

Input of tuning spin-dep. force
- Central: $^{4}_{\Lambda}$H & $^{7}_{\Lambda}$Li
- LS: $^{9}_{\Lambda}$Be

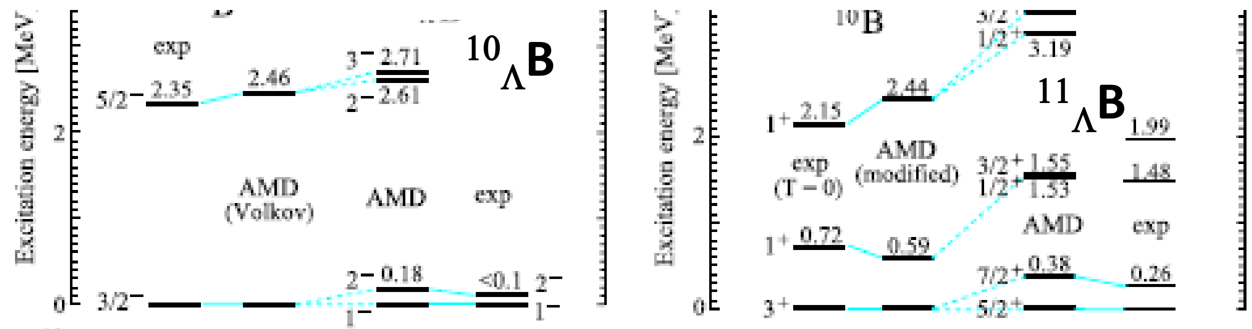


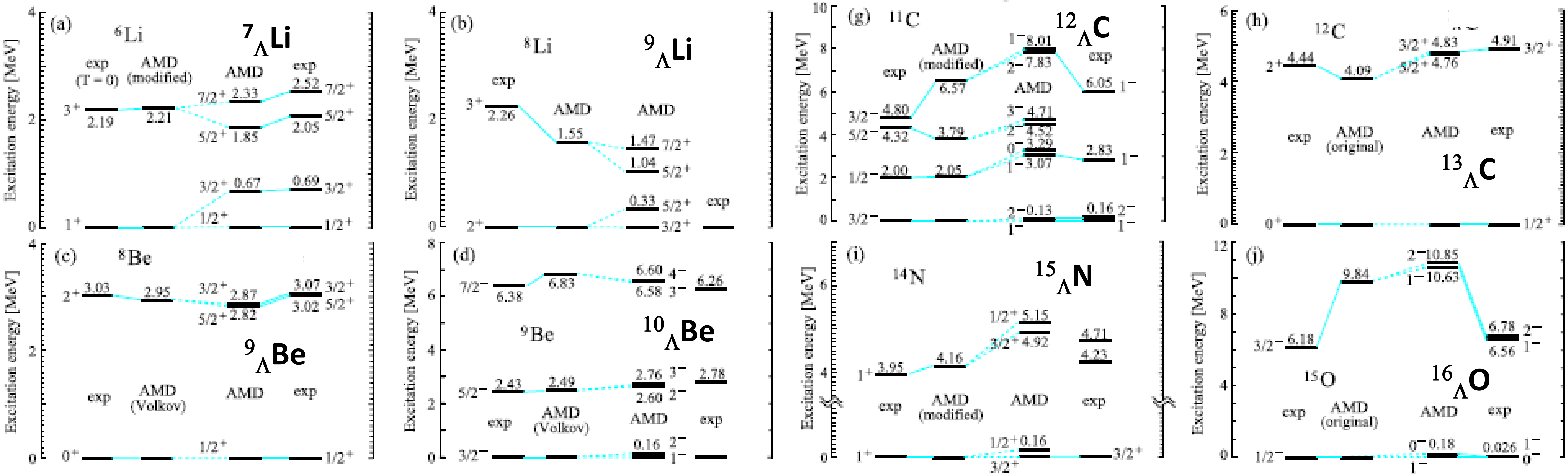


**Doublet ordering and spacing are mainly determined by ΛN spin-dep. force**

# An application to *sd*-shell Λ hypernuclei: $^{19}{}_{\Lambda}F$

**Spin-doublet is explained using common ΛN spin-dep. force in $^{19}{}_{\Lambda}F$**

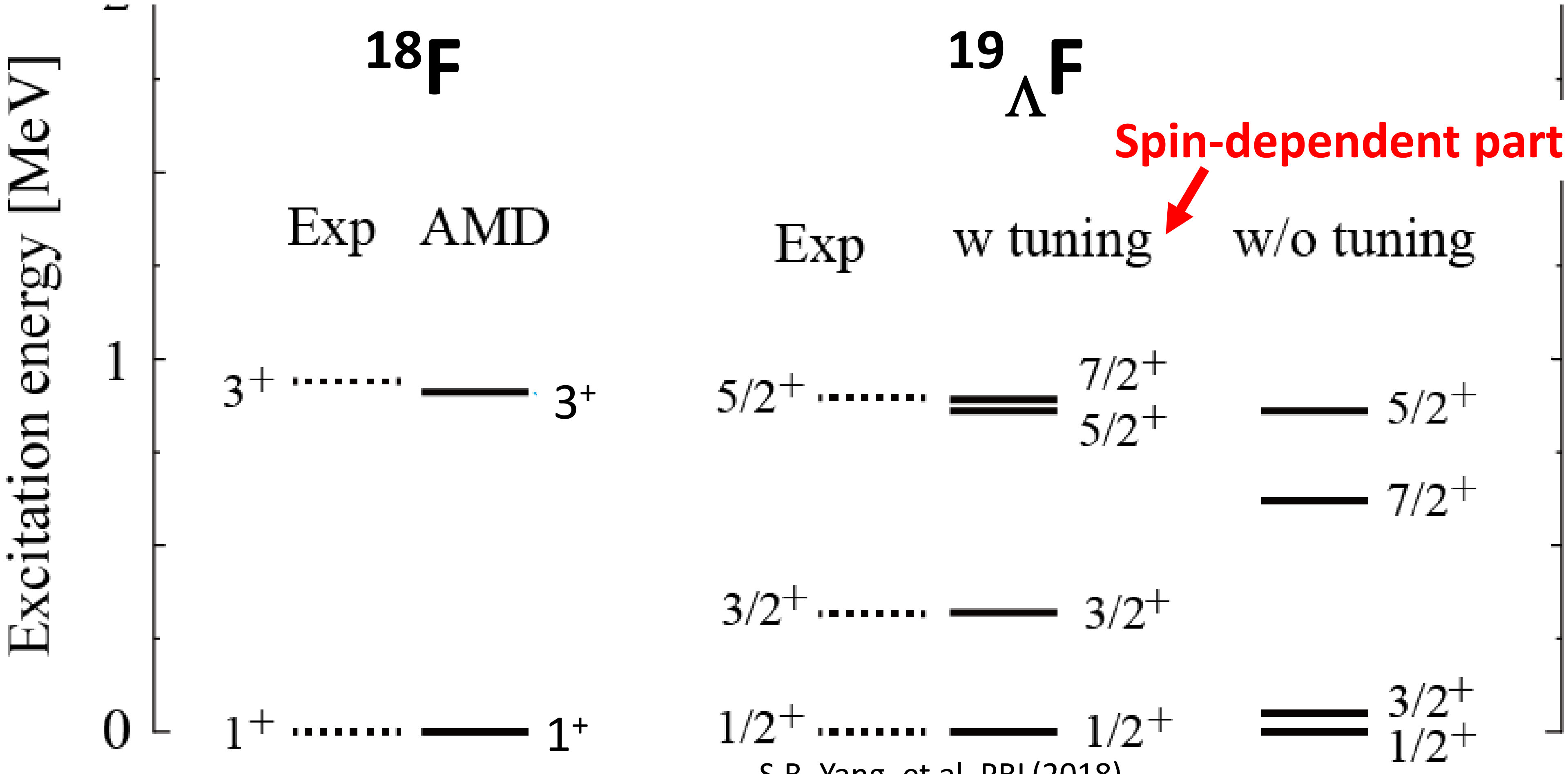


S.B. Yang, et al, PRL(2018)

**Ground-state doublet is consistent with recent J-PARC experiment using ΛN force tuned in $^{4}{}_{\Lambda}H$ & $^{7}{}_{\Lambda}Li$**

# Ξ hypernuclei

## "Application of HAL-QCD potential to $\Xi^- + {}^{14}N$ and prediction for ${}^{12}_{\Xi}Be$"

T. Tada, M. Isaka, M. Kimura, Y. Yamamoto

# Theoretical studies on YN interaction

## HAL-QCD ΛΛ and ΞN potential near physical q mass

Available online at www.sciencedirect.com

ScienceDirect

ELSEVIER

Check for updates

Nuclear Physics A 998 (2020) 121737

NUCLEAR PHYSICS A

www.elsevier.com/locate/nuclphysa

# ΛΛ and NΞ interactions from lattice QCD near the physical point

Kenji Sasaki [a,b,*], Sinya Aoki [a,b,c], Takumi Doi [b,d], Shinya Gongyo [b], Tetsuo Hatsuda [d,b], Yoichi Ikeda [e,b], Takashi Inoue [f,b], Takumi Iritani [b], Noriyoshi Ishii [e,b], Keiko Murano [e,b], Takaya Miyamoto [b]
(HAL QCD Collaboration)

# First principles ΞN potential from HAL QCD

- Even-parity(S-wave) ΞN potential Sasaki, et al. (HAL QCD Collab.), NPA**998**, 121737 (2020)

$$V(r) = \lambda_1 \mathcal{Y}(\rho_1, m_\pi, r) + \lambda_2 [\mathcal{Y}(\rho_2, m_\pi, r)]^2 + \sum_{i=1}^{3} \alpha_i \, e^{-r^2/\beta_i^2}$$

  - Short range repulsion: Gauss function
  - Long range part (meson exchange): Yukawa function

- HAL QCD ΞN potential has been applied to NNNΞ

  E. Hiyama, et al., PRL**124**, 092501(2020)

  ⇒ Very shallow binding was predicted

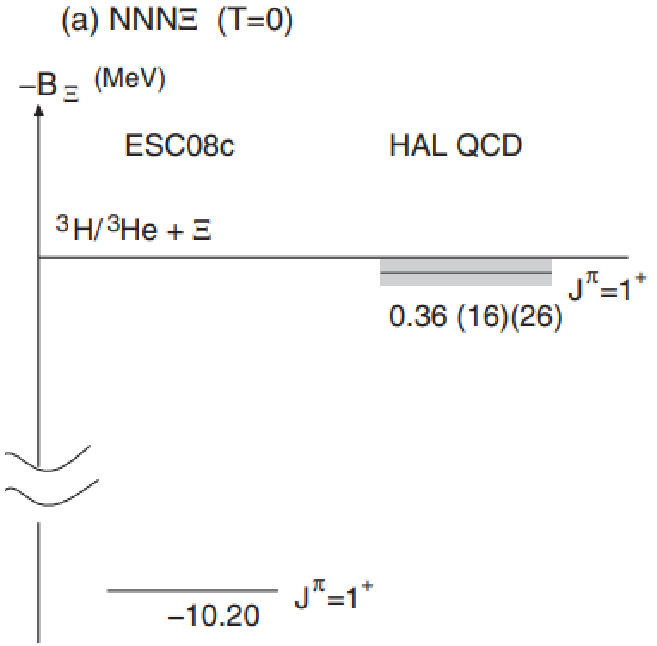


## Aim of this work

- We examine the HAL QCD potential applying to the $\Xi^- + {}^{14}N$ system
- We predict the $\Xi^- + {}^{11}B$ spectrum for the forthcoming experiment

# Modeling ΞN odd-parity potential

Odd-parity potential has not been derived by HAL QCD

Ansatz in this study

$$V(r) = \lambda_1 \mathcal{Y}(\rho_1, m_\pi, r) + \lambda_2 [\mathcal{Y}(\rho_2, m_\pi, r)]^2 + X \sum_{i=1}^{3} \alpha_i \, e^{-r^2/\beta_i^2}$$

- Long range part: Same as even-parity force (Wigner type)

  No S=-2 transfer by one-meson exchange ⇒ Winger term, even=odd

- Short range part: Unknown

  We assume the same potential as even-parity force, but multiply a factor X

  This factor is calibrated by the comparison with the recent exp. data

# Results: comparison with emulsion data of $\Xi^- + {}^{14}N$

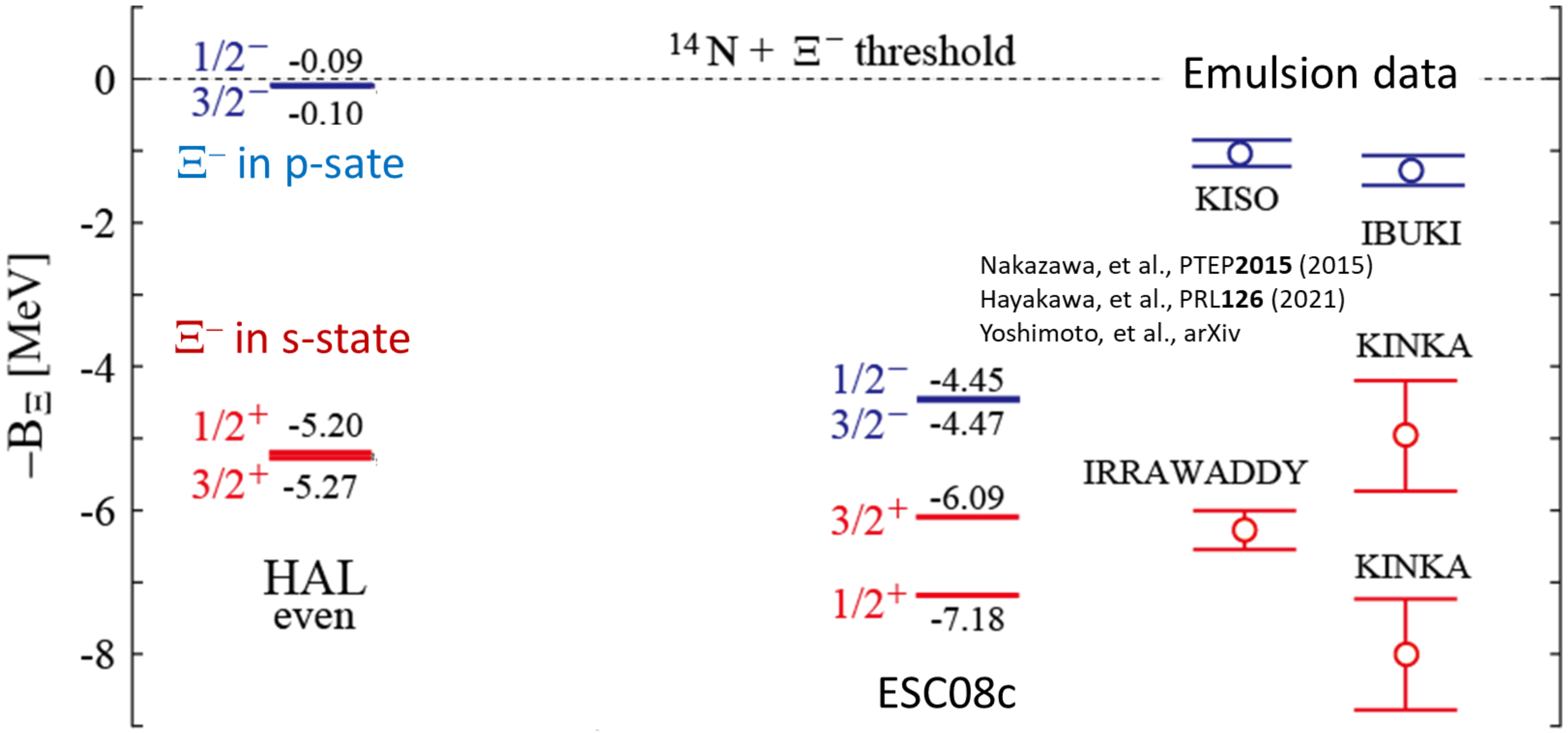


HAL QCD (only even-parity force) slightly underbound s- and p-wave states

# Results: comparison with emulsion data of $\Xi^- + {}^{14}N$

Odd-parity force: $V(r) = \lambda_1 \mathcal{Y}(\rho_1, m_\pi, r) + \lambda_2[\mathcal{Y}(\rho_2, m_\pi, r)]^2 + X \sum_{i=1}^{3} \alpha_i \, e^{-r^2/\beta_i^2}$

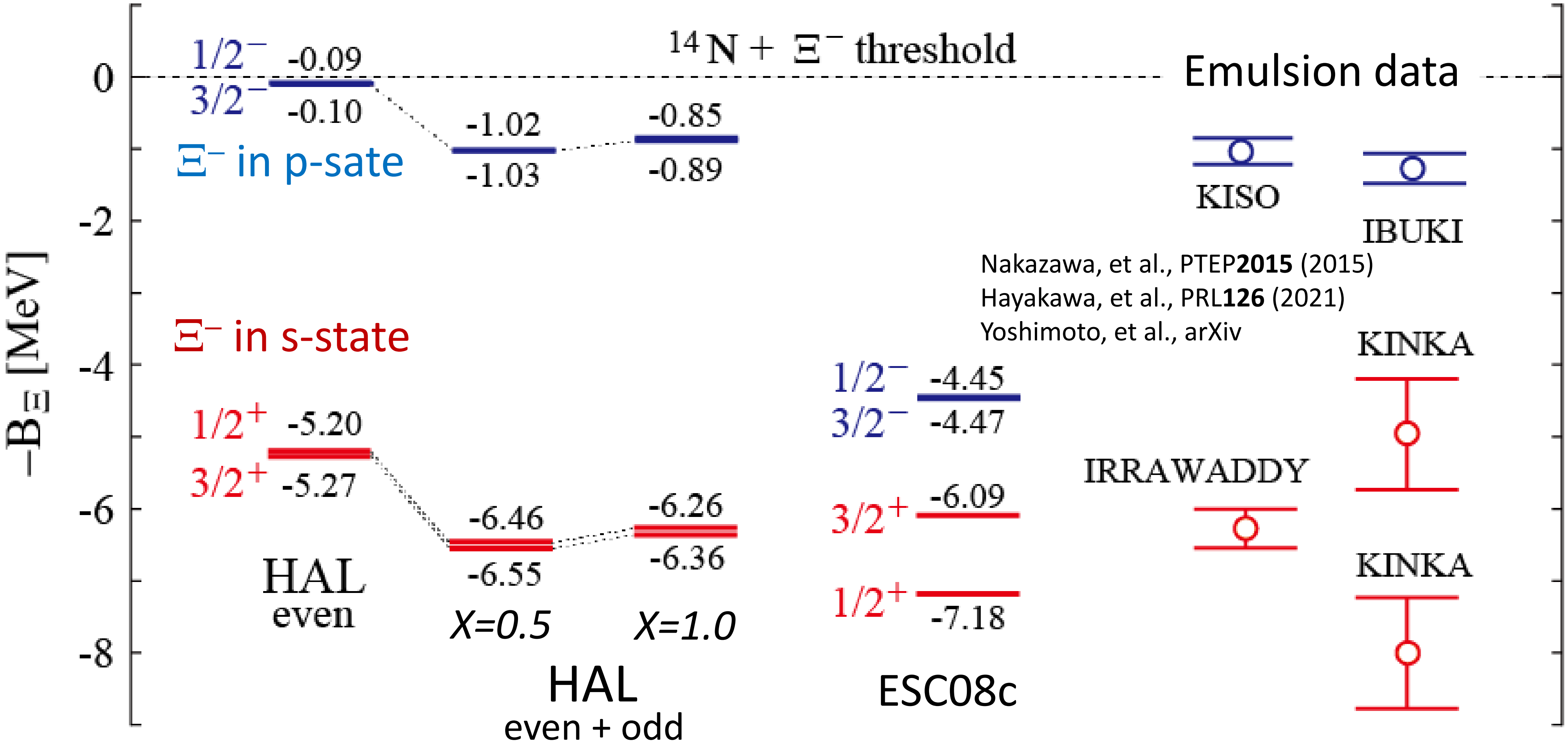


- $B_\Xi$ are consistent with exp by odd-parity force. Small uncertainty from short range part
- HAL QCD yields much smaller doublet splitting than Nijmegen potential ESC08c

# Results: Prediction for the $\Xi^- + {}^{11}B$ system (J-PARC E70)

High resolution ${}^{12}C(K^-, K^+){}^{12}_{\Xi}Be$ experiment planned at J-PARC

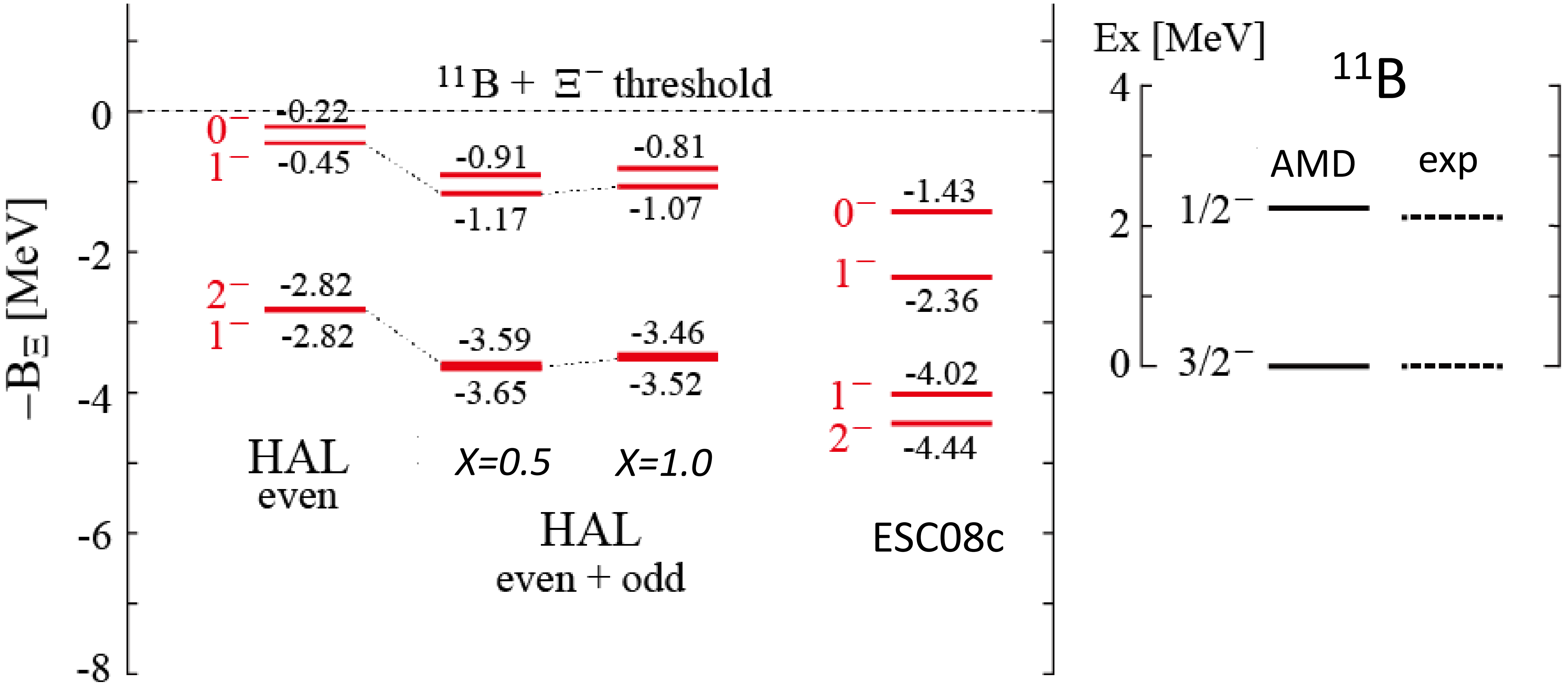


Calculated $B_\Xi$ is about 3.6 MeV for the ${}^{12}_{\Xi}Be$ ground state

# Results: $\Xi N$ -> $\Lambda\Lambda$ conversion width

$\Xi^- + {}^{14}N$ states ($\Xi^-$ in s state)

| Potential | $J^\pi$ | $B_\Xi$ [MeV] | Width [MeV] |
|---|---|---|---|
| HAL (even) | 1/2+ | 5.20 | 0.12 |
| | 3/2+ | 5.27 | 0.14 |
| ESC08c | 1/2+ | 7.18 | 1.79 |
| | 3/2+ | 6.09 | 1.94 |

narrow (HAL (even))

$\Xi^- + {}^{14}N$ states ($\Xi^-$ in p state)

| Potential | $J^\pi$ | $B_\Xi$ [MeV] | Width [MeV] |
|---|---|---|---|
| HAL (even) | 1/2- | 0.09 | 0.07 |
| | 3/2- | 0.10 | 0.07 |
| ESC08c | 1/2- | 4.45 | 1.64 |
| | 3/2- | 4.47 | 1.56 |

narrow (HAL (even))

$\Xi^- + {}^{11}B$ states ($\Xi^-$ in s state)

| Potential | $J^\pi$ | $B_\Xi$ [MeV] | Width [MeV] |
|---|---|---|---|
| HAL (even) | 1- | 2.82 | 0.12 |
| | 2- | 2.82 | 0.11 |
| ESC08c | 1- | 4.02 | 1.49 |
| | 2- | 4.44 | 1.43 |

narrow (HAL (even))

# Summary

- HyperAMD with G-matrix interactions is applied to $\Lambda$ and $\Xi$ hypernuclei
- $\Lambda$ hypernuclei: various $\Lambda$ hypernuclei, Nijmegen ESC potential
  - Mass dep. of $B_\Lambda$ is reproduced by describing core deformation
  - Doublet ordering and spacing are determined by $\Lambda N$ spin dependent force
- $\Xi$ hypernuclei: $\Xi^- + {}^{14}N$ and $\Xi^- + {}^{11}B$ states, HAL QCD $\Xi N$ potential

  By introducing phenomenological odd potential based on meson exchange picture,
  - KISO & IBUKI are reproduced and $B_\Xi$ for $\Xi_s$ is consistent with IRRAWADDY
  - Low-lying states of ${}^{12}_{\Xi}Be$ are predicted: $B_\Xi \simeq 3.6$ MeV for g.s.
- Future works:
  - $\Lambda$ hypernuclei: detailed analysis of ${}^{19}_{\Lambda}F$
  - $\Xi$ hypernuclei: level structure, production cross section